UNIVERSITY OF CALIFORNIA
RIVERSIDE

How Much is Enough? Addressing Data Gaps in Modeling PFAS Transport From Landfill Leachate Using MODFLOW 6

A Thesis submitted in partial satisfaction
of the requirements for the degree of

Master of Science

in

Chemical and Environmental Engineering

by

Clifford Anthony Button

June 2025

Thesis Committee:
Dr. Amanda Rupiper, Chairperson
Dr. Yujie Men
Dr. Don Collins

The Thesis of Clifford Anthony Button is approved:

_____

_____

_____

Committee Chairperson

University of California, Riverside

Acknowledgements

I would like to take this opportunity to thank my advisor, Amanda Rupiper, for being a supportive and engaging mentor to me for my academic journey at UCR. I thank you for having trust in me for wanting to do something different and helping me start a project from scratch.

Thank you to my thesis committee, Dr. Don Collins for sharing advice on how to go about the graduate program and looking towards the future as well as Dr. Yujie Men for all of her support and being able to review the thesis while away. I would also like to thank Dr. Georgios Karavalakis for being able to be a proxy for the thesis defense.

To my tribe, the Shoshone Bannock Tribes of Fort Hall Idaho, I thank them for their continuous support on my educational journey as well as their support over the years.

I want to thank the Native American Student Program for being my family away from home and for always having my best interest over the years.

To my supervisors and coworkers at Jurupa Community Services District for always having my best interest and being able to provide feedback on any of my academic projects.

Dedication

I dedicate my thesis work to my mom and dad who supported me every step of my educational journey, motivating me to always do my best on anything I do, and reminding me that the sky is the limit. To my sisters, Loreal and Alina, for being my cheerleaders throughout my academics and for letting me vent to them when I needed to.

I also dedicate this work to my grandmother and grandfather, Rose and Richard, for their continuous support and believing in me to go this far in academics. To my Cortez and Button family who encouraged me to continue in higher education and for always wishing me the best of luck.

To my graduate friends and classmates, John, Hovannes, and Matteo, for being my support group during this graduate program and for sharing words of encouragement and advice when times were rough especially on those late nights together.

To my friends, Sara, Neff, and Megan, for always having my best interest throughout this academic journey and for letting me vent when stress got the best of me.

To all of my other friends and family, thank you for your continuous support.

ABSTRACT OF THE THESIS

How Much is Enough? Addressing Data Gaps in Modeling PFAS Transport From Landfill Leachate Using MODFLOW 6

by

Clifford Anthony Button

Master of Science, Graduate Program in Chemical and Environmental Engineering
University of California, Riverside, June 2025
Dr. Amanda Rupiper, Chairperson

Per- and polyfluoroalkyl substances (PFAS) have been a topic of interest regarding the detrimental effects of exposure via drinking water and their persistence in the environment. PFAS are abundant in a variety of products such as cosmetics, food packaging, clothing and textiles, paints, and more. When these products reach the end of their lifecycle, they end up in landfills where they accumulate and can become new sources of PFAS in the form of leachate. As a result of this, landfills have been known to contaminate groundwater via leachate and degrade the water quality nearby.

This research aims to investigate the ability of using current/limited local, state, and federal data to create an accurate PFAS groundwater model using the Modular Finite-Difference Flow Model (MODFLOW) and assess any data gaps regarding modeling PFAS transport to help water providers identify sources of PFAS and estimate how long before a plume impacts their water supply. For the purpose of this study, the primary

source of PFAS is a municipal solid waste landfill. MODFLOW was used to simulate about 110 years' worth of groundwater flow and PFAS transport primarily focusing on PFOA and PFOS. The scenarios ran included (1) PFOA and PFOS transport with IDW interpolated initial concentrations, (2) PFOA and PFOS transport assuming an initial concentration of 0 ppt, (3) PFBS transport with IDW, Natural Neighbor, and Kriging interpolated initial concentrations and assuming an initial concentration of 0 ppt.

Table of Contents

List of Figures

List of Tables

1. Introduction

On April 10th 2024, the Environmental Protection Agency (EPA) established the first ever Maximum Contaminant Levels (MCLs) for six per- and polyfluoroalkyl substances (PFAS) in drinking water[1]. Public water systems (PWSs) have until 2029 to comply with these MCLs by implementing solutions to lower PFAS levels in drinking water that exceed these MCLs. The ability to keep PFAS levels below these MCLs is prompting concerns regarding possible violations, fines, and public notices.

PFAS are a group of fluorinated aliphatic chemicals that contain at least one carbon atom on which all of the hydrogen atoms are replaced by fluorine atoms[2]. PFAS have been manufactured in processes such as electrochemical fluorination and telomerization for various industries since the late 1940s[3]. Due to the high stability presented by the C–F bond, PFAS have continued to be an important component in the manufacturing of consumer products such as cosmetics, food packaging, paints, carpets, non-stick cookware, chrome-plating, textiles, etc[4–6]. Multiple C–F bonds make it difficult for microorganisms to biodegrade PFAS leading to long environmental residence times earning the name "forever chemicals." Over 3,000 types of PFAS exist, including short and long chain PFAS[7]. This number is expected to be much higher with the addition of new PFAS discovered recently such as Gen-X chemicals[8]. The abundance of PFAS in the environment paired with its ability to bioaccumulate in organisms has raised health concerns regarding exposure including potential links to certain cancers, reproductive and developmental issues, and more[9–11].

Municipal solid waste landfills (MSWLs) act as sources of PFAS. When PFAS-containing products reach the end of their lifecycle, they are sent to landfills for waste disposal. PFAS may leach from MSWLs contaminating groundwater over time, designating them as hot spots for PFAS investigations. PFAS in landfills can escape via volatilization or leaching into the groundwater[12,13]. While MSWLs take measures such as installing geomembrane liners, leachate management systems, and gas extraction wells to limit releases, these systems are not fail-proof and have been known to fail[14,15]. Leachate is defined as any water that has come into contact with solid materials such as trash or waste and has leached out some of its components. A study estimated about 600 kg/yr of PFAS mass in landfill leachate was collected in 2013 and sent to wastewater treatment plants for treatment[16]. The mass of PFAS in landfills is expected to increase due to growing waste generation from population increases and higher consumption rates.

With the risk of PFAS contaminating the groundwater, groundwater modeling has been one of many solutions in predicting, assessing and understanding groundwater flow, quality, sustainability, and contaminant transport related to PFAS. Only a handful of studies have been done regarding groundwater modeling, specifically on PFAS transport using programs like Modular Finite-Difference Flow Model (MODFLOW). Though these studies focus on a variety of scenarios such as modeling on a watershed scale, estimating historical PFAS loads, and understanding PFAS precursor transformation, there are very few that have modeled scenarios for landfills.[17–19]

This case study aims to understand PFAS transport in landfill leachate its fate in groundwater systems, examine the availability of local, state, and federal data and its impact on groundwater model development, all of which may impact PWSs on or after 2029, and assess the efficiency of different interpolation methods when there is an absence of data.

2. Methodology

2.1 Study Area

The study area focuses on the El Sobrante Landfill located in the northeastern portion of Temescal Valley, California (CA) and is approximately 2.5 miles southwest of Lake Mathews and 1.5 miles east of Interstate 15 illustrated in Figure 1. The study area is within the Santa Ana River Basin and is upgradient from the Bedford-Coldwater and Elsinore Valley subbasins. The landfill has been operating since 1986 and has the capacity to process about 70,000 tons of waste per week, accounting for 43% of Riverside County's annual waste[20].

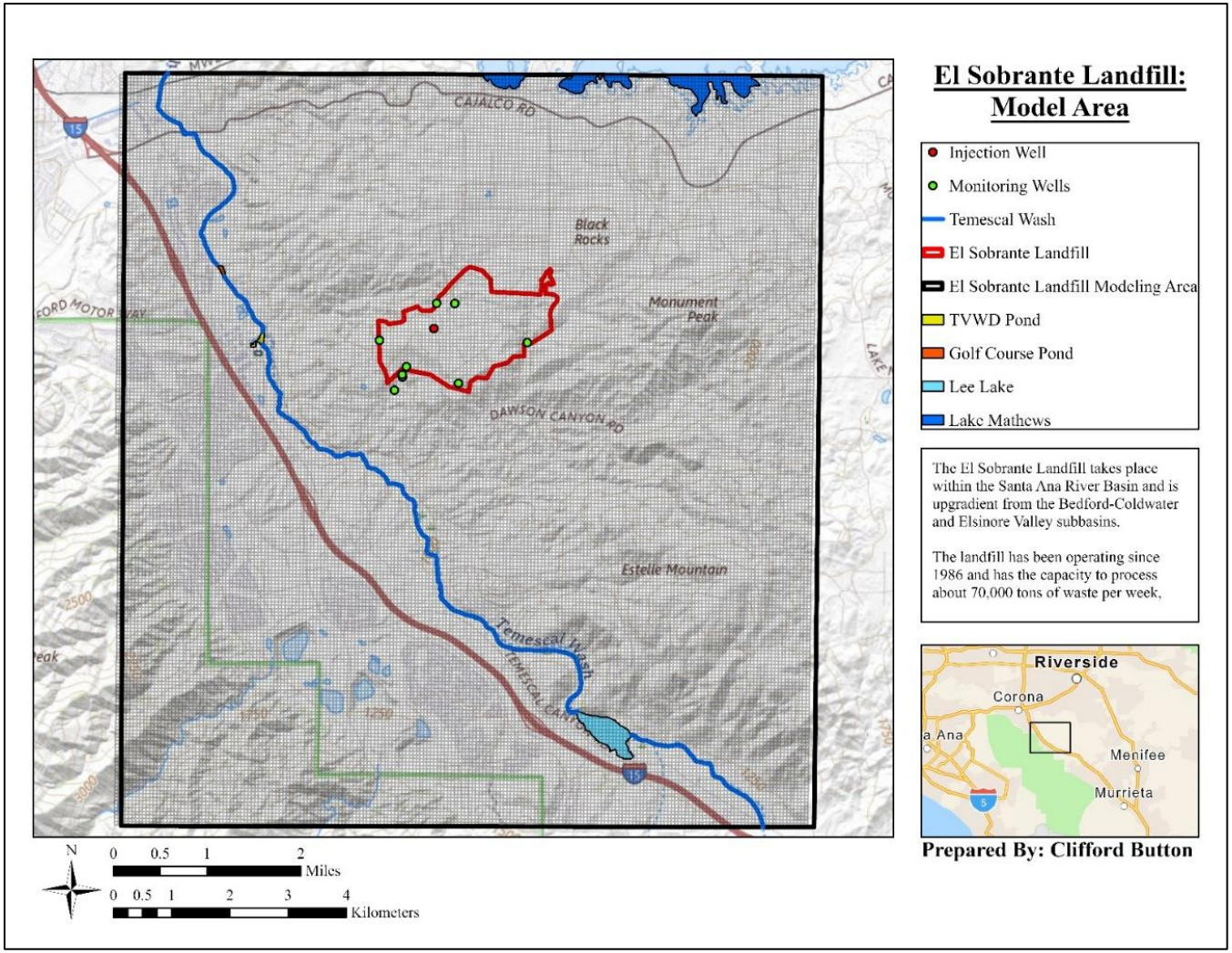

Figure 1. Top view of the modeling area including but not limited to Temescal Valley, PFAS monitoring wells, Temescal Wash, the El Sobrante Landfill and the cell grid consisting of 211,800 cells represented by each small square of the grid

2.2 Data Collection & Refinement

Data was sourced from a variety of local, state, and federal resources to assign model parameters in MODFLOW dating from 2017–2024 as described in Table X.

2.3 Digital Elevation Models & Aquifer Characteristics

Ground level data was gathered from Digital Elevation Models (DEM) from the United States Geological Survey (USGS) National Map - Data Delivery and was necessary to establish the top geological layer in MODFLOW to serve as a basis for categorizing subsequent bottom layers in the model[21]. The ground level elevation profile can be seen in Figure 2.

Groundwater elevation data was retrieved from CA's Sustainable Groundwater Management Act (SGMA) Groundwater Live website which was required to assign an initial head to the model. Annual data spanning from 2017–2024 was documented focusing on available data for months prior to June to account for CA's wet season when aquifers are generally replenished[22]. CA's Well Completion Reports (WCR) database was utilized to gather data regarding geographical coordinates, well depths, depth to water, and soil profiles[23]. The soil profiles were used specifically for hydraulic conductivity, porosity, and layer characterization. Specific values for porosity and hydraulic conductivity were found using StructX which is a collection of information related to a variety of structural engineering parameters and information[24].

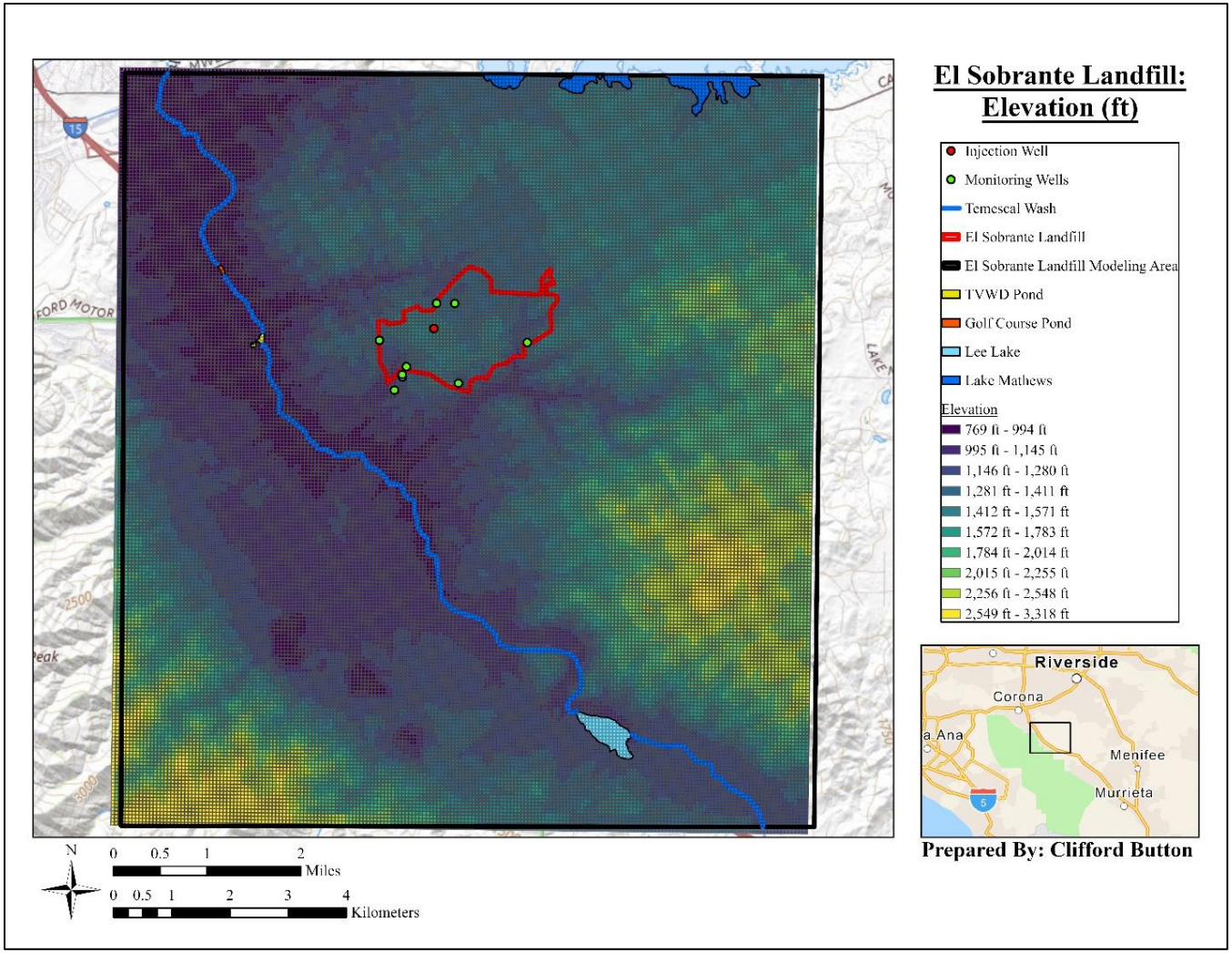

Figure 2. Ground level elevation map of the study area in feet. The highest and lowest elevations of the study area were 3,318 ft and 769 ft, respectively. The lowest elevations reflect Temescal Creek, whereas the highest elevations reflect the mountains.

In this case, information related to soil characteristics (hydraulic conductivity and porosity values) were gathered from there. In combination with the WCRs, this data was used to assign hydraulic conductivity and porosity values using Equation 1[25–27]. Soil profiles were categorized into five layers and based on the majority of the composition of the soil type, that soil type was assigned to each layer at that well location. This data was transferred to ArcGIS Pro where it was interpolated using Equation 1 across the model area to represent heterogeneity of actual soils across the layers using Kriging interpolation:

$$\hat{Z}(s_0) = \sum_{i=1}^{N} \lambda_i Z(s_i) \quad (1)$$

where, $Z(s_i)$ is the measured value at the ith location, λ_i is an unknown weight that must be calculated during the interpolation process for the measured value at the ith location, s_0 is the prediction location and N is the number of measured values[28]. This method was also applied to porosity, resulting in five files each for hydraulic conductivity and porosity. Figure 3 and Figure 4 illustrate the hydraulic conductivity and porosity of the first layer, respectively.

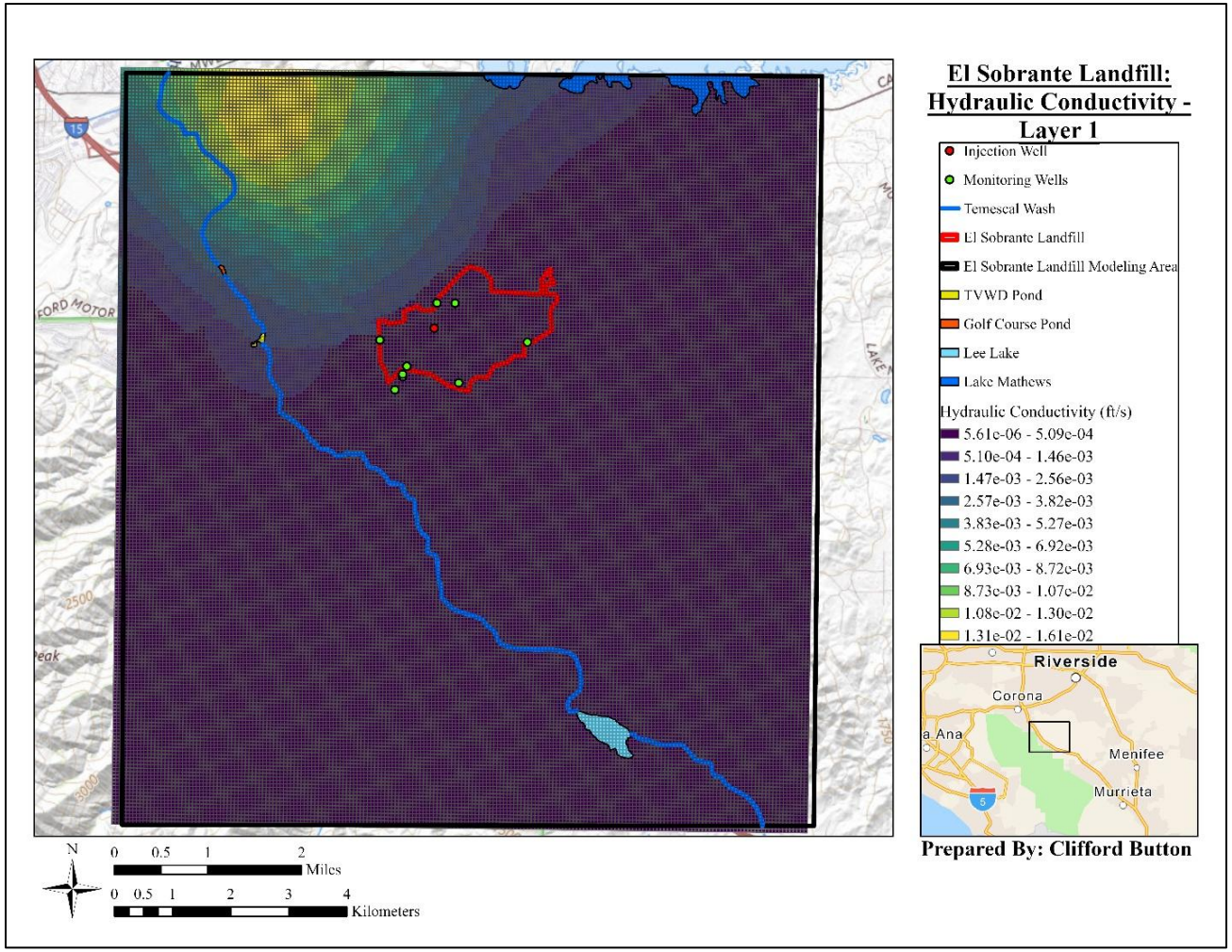

Figure 3. Hydraulic conductivity of the first layer ranges from 5.61E-3 (denoted as purple) to 1.61E-2 ft/s (shown as yellow). Higher values indicate greater permeability, whereas lower values indicate reduced permeability. Kriging interpolation was used to create a heterogeneous profile using data from the CA WCR database.

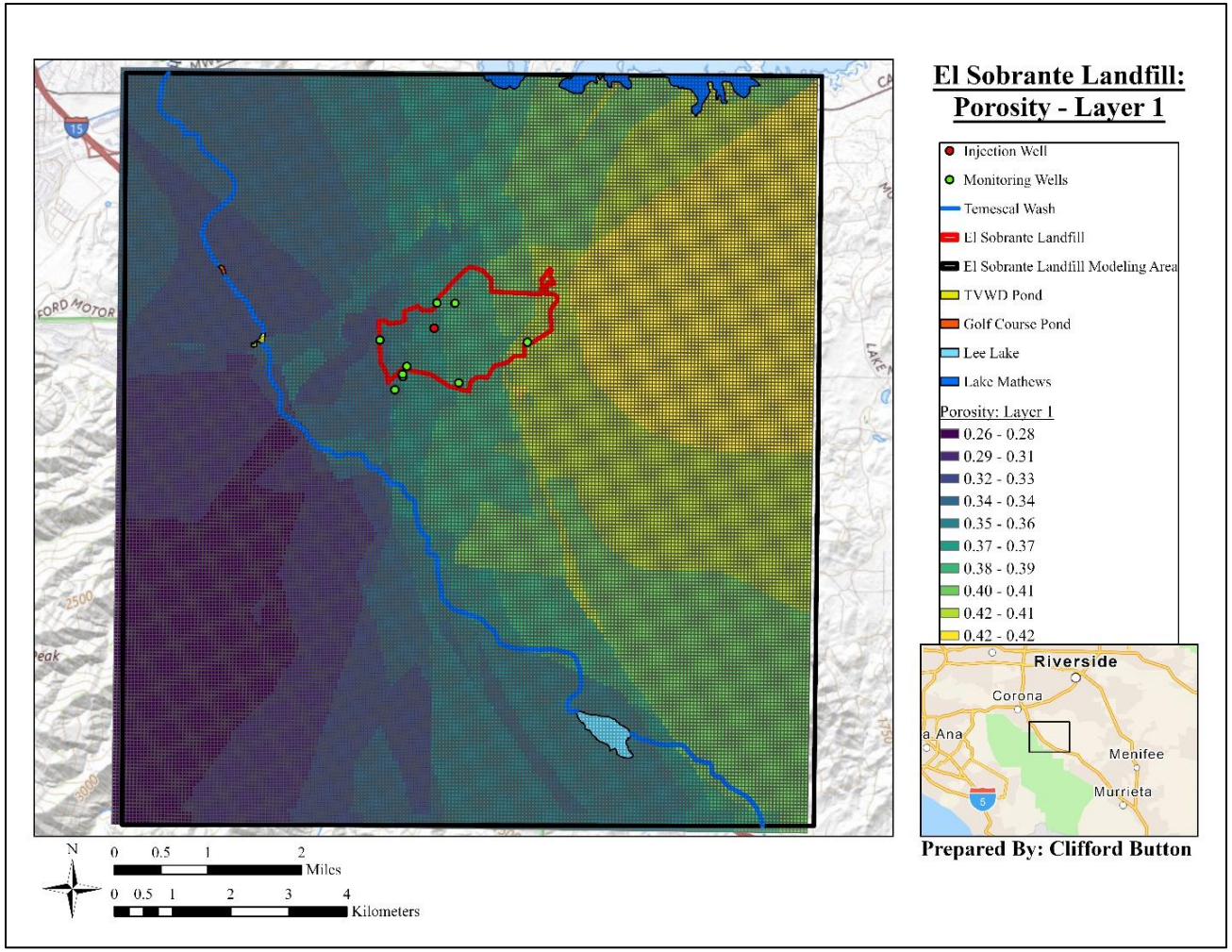

Figure 4. Porosity values of the first layer in the model where the highest and lowest values are 0.42 and 0.26, respectively. The highest values are located in the northeastern portion of the study area. Kriging interpolation was used to create a heterogeneous profile using data from the CA WCR database. Porosity was used to find retardation factors in MODFLOW.

2.3 Surface Waters

The model consists of 5 water bodies which are referenced in Figure 1: Lake Mathews, Lee Lake (Corona Lake), Temescal Creek, and two smaller ponds along Temescal Creek. Two USGS monitoring stations along Temescal Creek were used to obtain data regarding daily gage heights and depths of both Temescal River and Lake Corona for years 2017–2024[29,30].The average of all daily gage heights and depths for each year were calculated to represent a single value for each year and assigned to each of the water bodies except Lake Mathews. Data on Lake Mathews was gathered from Snoflo, a website containing climate and outdoor recreation data including snowfall/snowpack, streamflow monitoring, river and creek levels, and dam storage level data[31]. Due to the limited data on Lake Mathews (2 years' worth), the lake levels for the 7 years were assumed to be constant at 1,370 ft. Data for each of these water bodies is summarized in Table 1.

Table 1. Water depths and pool elevations represented in feet to set hydraulic heads for different surface waters in MODFLOW. Data was sourced annually from the USGS and Snoflo from 2017–2024, specifically from April–March rather than January–December.

Year	Temescal Creek Depth (ft)	Golf Course Pond Depth (ft)	TVWD Pond Depth (ft)	Lee Lake Depth (ft)	Lake Mathews Pool Elevation (ft)
2017	2.12	2.12	2.12	25.57	1,370
2018	2.26	2.26	2.26	24.09	1,370
2019	2.28	2.28	2.28	28.28	1,370
2020	2.21	2.21	2.21	27.34	1,370
2021	2.19	2.19	2.19	22.94	1,370
2022	2.37	2.37	2.37	24.83	1,370
2023	2.52	2.52	2.52	28.91	1,370
2024	2.36	2.36	2.36	30.98	1,370

2.4 Precipitation

Precipitation data was downloaded from the Riverside Flood Control and Water Conservation District consisting of annual data[32]. Data was sorted in Excel where the timeframe was from April 2017 – March 2025 and an average of rainfall was calculated for each year as shown in Table X. Data for January – March 2025 were missing, so an average of the previous 9 months were taken to represent April 2024 – March 2025.

Table 2. Annual precipitation data for 2017–2024 in in/yr. Data was sourced from the Riverside Flood Control and Water Conservation District which represented the Santa Ana Watershed rather than just the study area.

Year	Rainfall (ft/sec)	Annual Precipitation (in/yr)
2017	1.22E-08	4.61
2018	5.21E-08	19.72
2019	3.37E-08	12.77
2020	2.56E-08	9.68
2021	2.46E-08	9.31
2022	6.11E-08	23.12
2023	4.67E-08	17.69
2024	2.64E-09	1.00

2.5 PFAS

PFAS data was gathered from both GeoTracker and the Groundwater Ambient Monitoring Assessment (GAMA) databases[33,34]. Data was uploaded into R Studio and sorted for specific PFAS type and by year from 2017–2024. They were further sorted for samples with a location ID of El Sobrante Landfill and divided into two categories: leachate samples and monitoring well samples. There was a total of 10 wells: 9 monitoring and 1 injection. In this study, the injection well is defined as the source of leachate entering the groundwater. All of these wells can be referenced in Figure 1. The location of the injection well assumes that the majority of samples have the highest concentrations there and the highest possibility of being a point source of leachate spills.

Leachate and monitoring well samples were taken in 2017 and/or 2022. The PFAS types focused on this landfill and the highest concentrations reported for each one is summarized in Table 3. These concentrations were assigned to the injection well as a starting point for leachate flow rates.

Table 3. PFAS of interest, maximum concentrations reported in the leachate collection and removal system at the landfill, and the proposed MCLs in parts per trillion (ppt). Concentrations were sourced from CA's GeoTracker and GAMA databases for 2017 and 2022.

PFAS Type	Max Concentration (ppt)	EPA MCL (ppt)
PFHxA	51,000	NA
PFOA	26,000	4.0
PFBA	18,000	NA
5:3FTCA	17,000	NA
PFBS	5,200	NA
PFHxS	770	10
PFOS	230	4.0
PFNA	180	10

2.6 Leachate

In the context of this research, leachate is water that has come into contact with municipal solid waste and has retained some of its constituents as it has percolated from rainfall or other liquids present. Using documentation from the landfill's annual reports spanning from 2017–2023, data regarding the leachate collection and removal system (LCRS) was collected from October–March of each year (6 months) for years 2017–2022 and/or the full year from March–April[35–41]. Leachate volumes were added together to create a total volume representing an entire year rather than 6 months; however, volumes after 2022 remained constant as a result of unavailable data. In combination with annual rainfall data, leachate volumes were plotted together to show the correlation between precipitation and leachate generation as shown in Figure 5.

The year with the highest recorded leachate volume was 2021 with 4,500,530 gallons collected from the LCRS, whereas 2022 had the highest rainfall of 23.12 inches. 2023 and 2024 are both questionable due to the lack of data available.

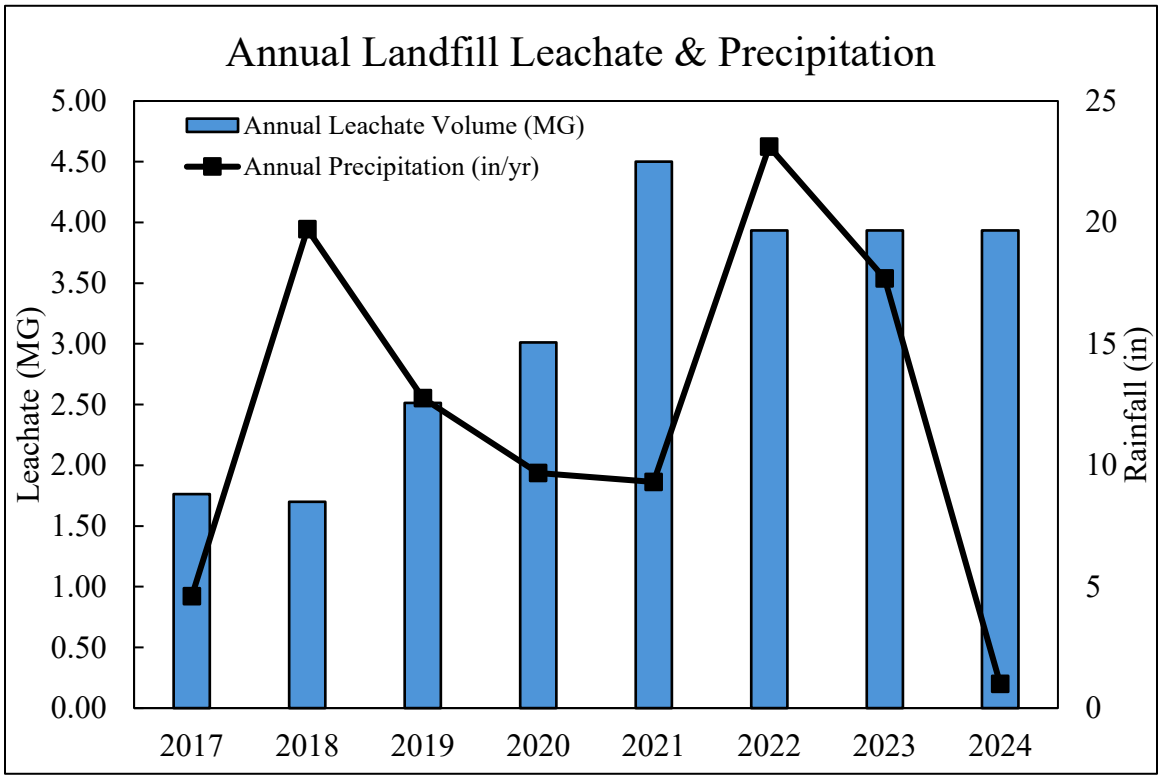

Figure 5. Annual leachate volume reported in a million gallons (MG) at the El Sobrante Landfill plotted with the annual precipitation recorded for years 2017–2024. From 2017–2020 there is a correlation between the amount of rainfall and the leachate being generated; however, after 2020 there is a lag between the increased rainfall and the leachate which could be from assuming an average rainfall for the whole year.

Landfill liners are barriers in landfills that prevent waste and leachate from entering and contaminating the groundwater below them. These landfill liners are made up of either clay or geomembranes and have a capture efficiency of 98-100% meaning that 1-2% of waste and leachate aren't captured[42].

Leachate volumes that were not captured by the liner were calculated using the annual total volumes and the liner inefficiency as shown in Table 4.

Table 4. Annual volumes of leachate, liner capture efficiency, and leachate rates taken from the El Sobrante Landfill Annual Reports. The leachate rates in ft^3/s were inputted into MODFLOW for unit consistency.

Year	Total Leachate Volume (MG)	Capture Efficiency of Liner (%)	Leachate Not Captured (gal/yr)	Leachate Rate (gal/day)	Leachate Rate (ft^3/s)
2017	1.76	0.98	35,255.76	96.59	1.49E-04
2018	1.70	0.98	33,991.92	96.59	1.49E-04
2019	2.51	0.98	50,286.50	93.13	1.44E-04
2020	3.01	0.98	60,232.32	137.77	2.13E-04
2021	4.50	0.98	90,010.60	165.02	2.55E-04
2022	3.93	0.98	78,685.38	246.60	3.82E-04
2023	3.93	0.98	78,685.38	215.58	3.34E-04
2024	3.70	0.98	78,685.38	215.58	3.34E-04

The volumes of leachate not captured were converted into flow rates to determine annual leachate rates of infiltrating the local groundwater as shown in Table 4. These annual rates were used for assigning injection rates in ft^3/s for the injection well in the model for PFAS.

2.7 Computational Modeling

2.7.1 MODFLOW 6

MODFLOW is a modular hydrologic model created by the USGS and is considered an international standard for simulation and predicting a variety of groundwater conditions and groundwater/surface–water interactions[43,44]. The current version is MODFLOW 6 and it was developed to support multiple models and types of models within the same simulation. For this research, the hydrologic model used in MODFLOW 6 was the Groundwater Flow Model (GWF) which simulates three–dimensional,

transient, groundwater flow. It is based on a generalized control–volume finite–difference (CVFD) approach where a cell can be hydraulically connected to any number of nearby cells. The graphical user interface (GUI) used for MODFLOW 6 in this research is ModelMuse[45].

2.7.2 Model Setup

The model is made up of 199 columns, 215 rows, 211,800 cells (nodes), and 5 layers. The simulation was composed of 14 stress periods and broken into 1-to-12-time steps. Stress periods represented 1 month, 1 year and, 20 years in some cases as shown in Table 5. In contrast, time steps represented months or years and were just smaller increments of stress periods as described in the next few sentences. A stress period is the simulation time broken up into separate periods and subdivided into time steps. In this case, Time steps are smaller units of time in the simulation aimed at numerical stability and accuracy. In a stress period, the parameters such as groundwater pumping are held constant until the next stress period begins, whereas groundwater flow equations are solved at each time step. Table 5 shows a breakdown of the stress periods and time steps in regard to time spans. Stress periods 1, 10–14 each represents steady state where stress period 1 establishes initial conditions. All other stress periods represent transient conditions. 12 months were chosen during the calibration and validation because data was known for the years of 2017 – 2024; however, all of the time after 2024 are to project into the future for which the data is unknown.

Table 5. Stress periods and time steps of the simulation for calibration, validation, and PFAS transport runs. 20 years were used for the time steps after 2024 because PFAS moves slowly over time in some cases and it helped understand long term transport of PFAS in groundwater.

Year	Stress Period	Time Steps	Time Span of Stress Period
2017	1	1	1 month
2017	2	12	12 months
2018	3	12	12 months
2019	4	12	12 months
2020	5	12	12 months
2021	6	12	12 months
2022	7	12	12 months
2023	8	12	12 months
2024	9	12	12 months
2045	10	4	20 years
2065	11	4	20 years
2085	12	4	20 years
2105	13	4	20 years
2125	14	4	20 years

The local aquifer was assumed to be unconfined, where the water table is at atmospheric pressure and the groundwater levels are able to fluctuate based on recharge and pumping. It was also assumed that groundwater pumping and groundwater recharge via recycled water and recharge basins did not occur in the model due to unavailable data.

MODFLOW 6 uses a variety of packages which define specific types of inputs for specific processes and are utilized by models such as GWF in this study. A breakdown of the packages used, definitions, and parameters that were assigned to each one is summarized in Table 6.

Table 6. MODFLOW packages utilized in the simulations for calibration, validation, and transport runs

MODFLOW Packages & Datasets	Purpose	Parameters Assigned	Source
Hydrology	Assign Kx, Ky, and Kz to the 5 layers in the model	Kx, Ky, Kz	WCRs
Hydrology	Assign η to the 5 layers in the model	η	WCRs
Modflow_Initial_Head		Measured Heads	SGMA
Specific Storage	Assign data to the specific storage	SS	Default
Specific Yield	Assign data to the specific yield	SY	Default
MT3D – USGS	Simulates solute transport for a single chemical species	PFAS Concentrations	GAMA & GeoTracker
RCH	Assign precipitation data	Precipitation	USGS
GHB	Assign boundary heads and conductance to water bodies	Boundary Heads, Conductance	USGS
RIV	Assign river stage, conductance, and river bottom data	River Stage, Conductance, River Bottom	USGS
WEL	Assign injection rates for leachate	Injection Rates	El Sobrante Landfill Annual Reports
OBS	Assign observed data for calibration	Measured Heads	SGMA

2.7.3 Calibration & Validation

Using the previous data on groundwater levels, 24 observation wells were created to monitor predicted changes in hydraulic head and concentrations in the model. The groundwater level measurements were taken from the same source as the initial head profile, SGMA Groundwater Levels, which can be seen in Figure 6.

Because the beginning of the simulation starts in April of 2017, the majority of measurements were chosen in April of each year starting from 2017-2024; however, for wells that did not have data for the month of April, the next closest recorded measurement was chosen ranging from February-May. Although each well had 8 measurements recorded for each year totaling 192 observation points, only 145 (76%) of them were usable due to incomplete records of measurements.

In MODFLOW, calibration is supported by using the Parameter ESTimation (PEST) software which automatically estimates parameters and calibrates groundwater models[46]. It modifies the parameters of interest so that the simulated observations are closer to matching up with the measured observations. Ideally, the overall prediction uncertainty in the model will be reduced via measured and simulated observations closely matching. However, by forcing observations to match up more closely, the risk of overfitting the model increases substantially[47].

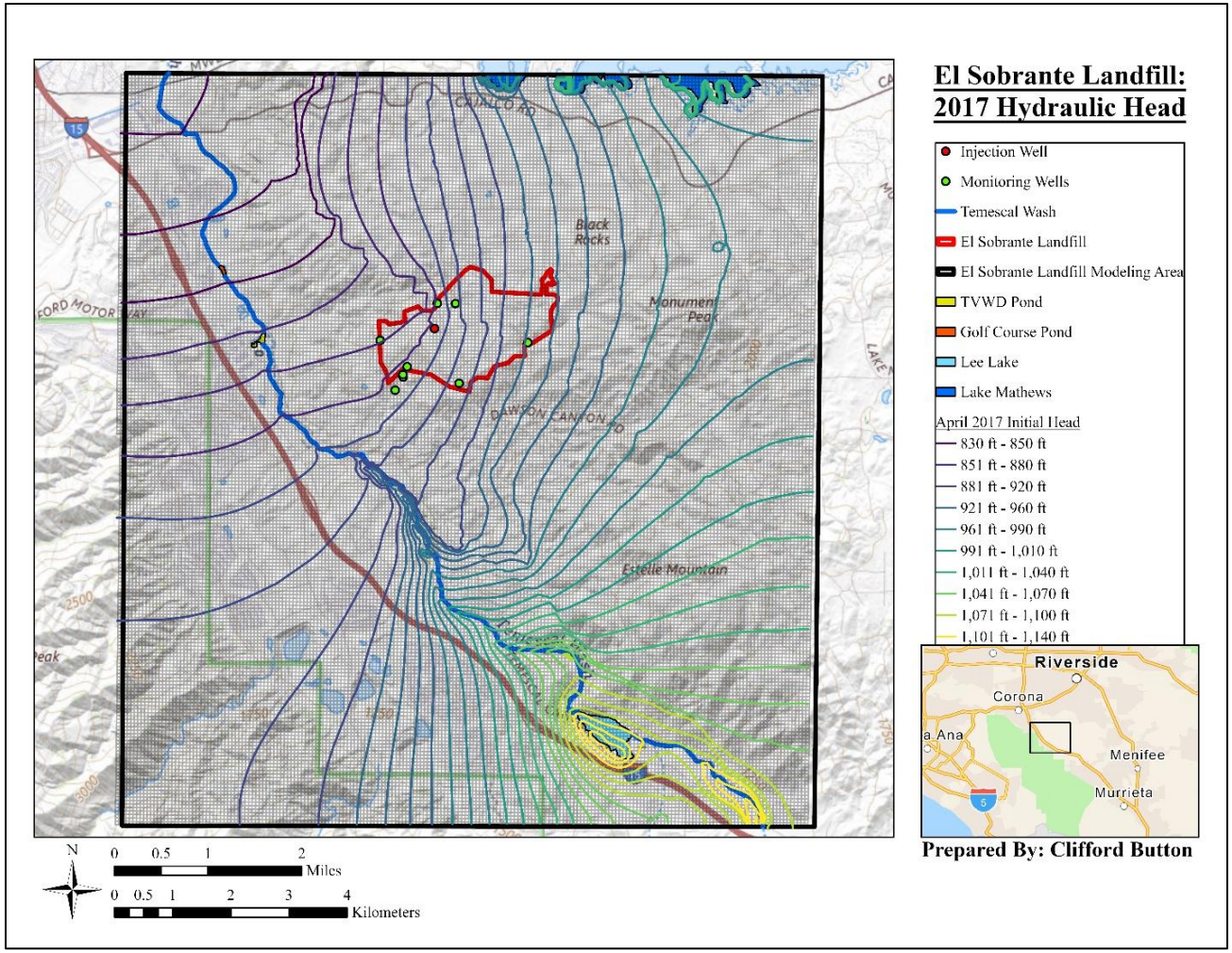

Figure 6. MODFLOW output of the 2017 hydraulic head represented in ft. The hydraulic gradient shifts towards the northwestern part of the map towards the Santa Ana River. Data for groundwater levels was sourced from the CA SGMA database where the initial profile was interpolated using kriging interpolation as a starting point for MODFLOW.

PEST uses the nonlinear estimation method, Gauss-Marquardt Levenberg, which solves nonlinear least squares problems for numerical optimization. This algorithm, in PEST, combines the Gauss-Newton method and the gradient descent method which are both numerical minimization algorithms. The gradient descent method reduces the sum of squared errors by updating the coefficients in the direction of the steepest descent, whereas the Gauss–Newton method reduces the sum of squared errors by assuming that the least squares function is locally quadratic in the coefficients and then finding the minimum of that quadratic approximation[48]. Using this method allows for fewer model simulations, resulting in short run times.

Parameters that were calibrated included hydraulic conductivity for each of the layers (5 total), specific storage, specific yield, and the conductance of Lake Mathews, Lake Corona, Temescal Creek, and the two ponds. Estimated values for these parameters are summarized in Table 7 for initial guess and 2 calibration simulations.

Table 7. Calibrated parameters using PEST. Calibration #1 was simulated for 2017–2019, whereas calibration #2 was simulated for 2017–2020. An extra year was simulated for calibration #2 due to increased hydraulic head percent errors as described in Figure 7.

PEST Parameter	Initial Value	Calibration #1 Value	Calibration #2 Value
Specific Storage (ft^{-1})	0.001	4.30E-09	1.02E-06
Specific Yield (unitless)	0.2	0.285	0.12
Lake Mathews Conductance (ft^2/s)	1.00E-05	4.30E-09	3.33E-06
Lake Corona Conductance (ft^2/s)	0.004	5.60E-04	1.33E-03
TVWD Pond Conductance (ft^2/s)	0.004	5.60E-04	1.33E-03
Golf Course Pond Conductance (ft^2/s)	0.004	5.60E-04	1.33E-03
Temescal Creek Conductance (ft^2/s)	0.01	5.68E-03	6.06E-03

The parameters that had the most variability were the specific storage and the conductance of Lake Mathews with 3 or more orders of magnitude.

The groundwater model used 2 calibration runs, Calibration #1 and Calibration #2, and were simulated for the years 2017- 2019 and 2017-2020, respectively. After calibrating for a second time, the model was validated for years 2017-2024. Figures 7 and 8 illustrate boxplots of the groundwater head percent errors for the 24 observation wells of the initial, calibration, and validation runs.

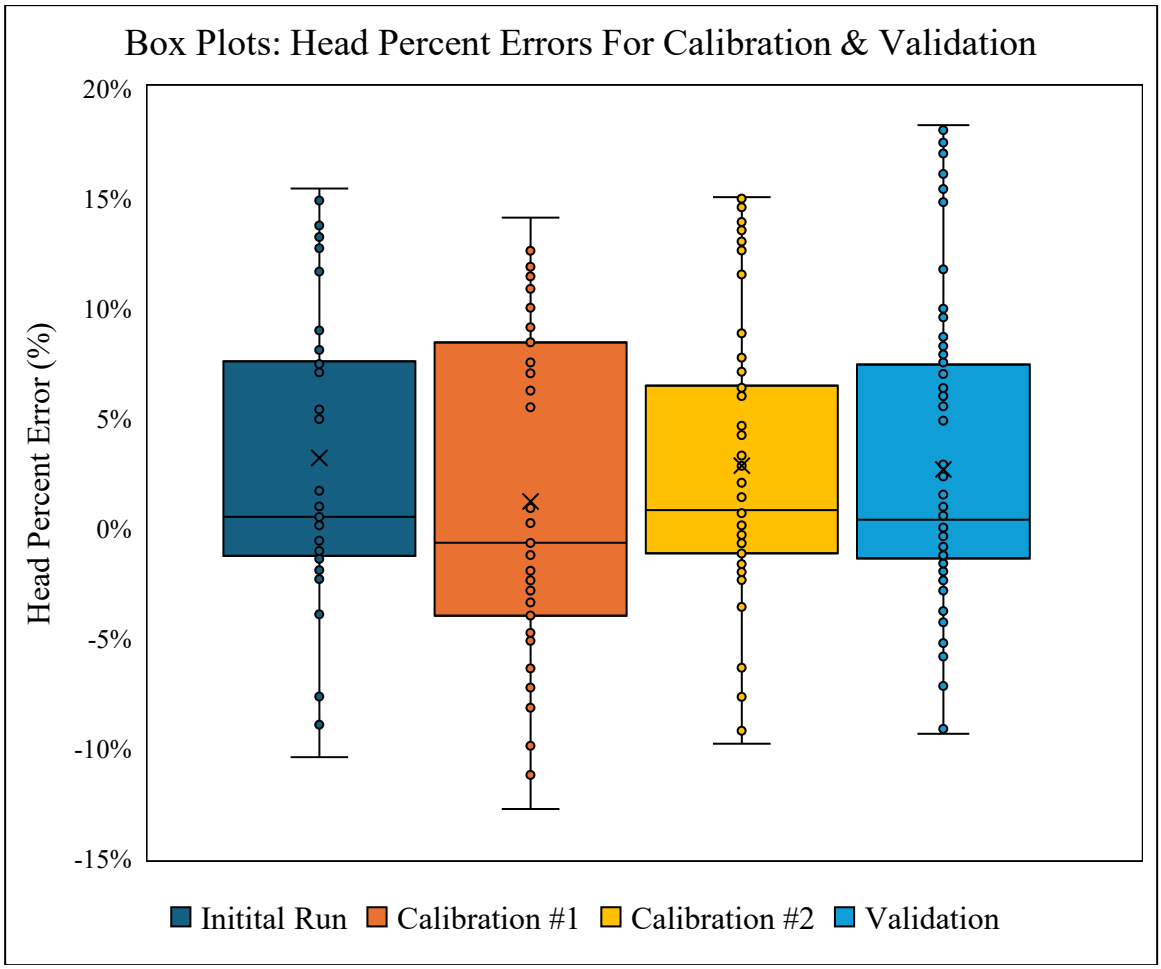

Figure 7. Box plots representing the percent errors of each simulation of groundwater hydraulic heads from the Initial Run (2017-2019), Calibration #1 (2017-2019), Calibration #2 (2017-2020), and Validation (2017-2024) simulations. Percent errors increased after the first calibration run which prompted another calibration run.

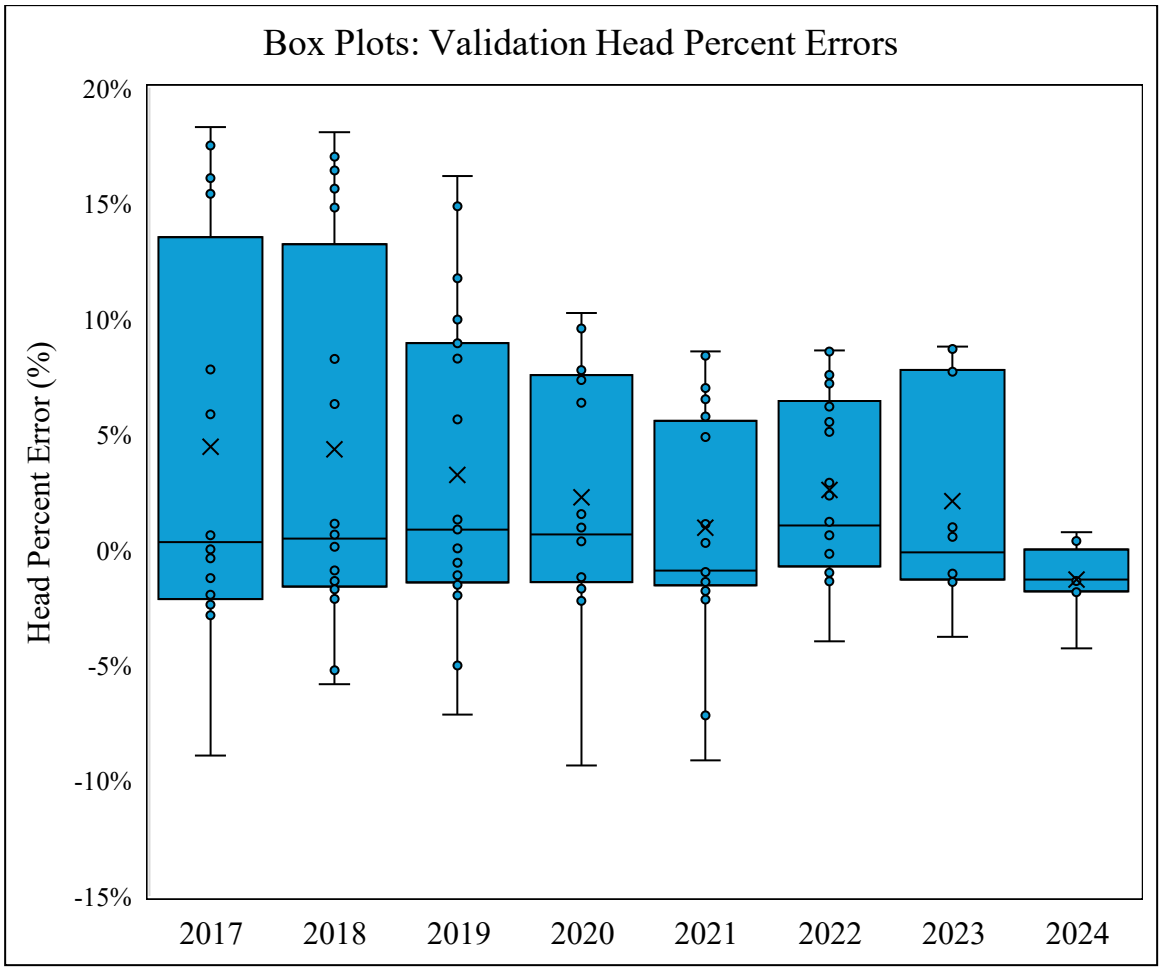

Figure 8. Box plots representing the individual percent errors of simulated groundwater hydraulic heads for the Validation run (2017-2024). The overall error shrunk over time most likely due to the decreased number of observations over time.

The validation was stable and there weren't any observed drifts or trends in higher or lower hydraulic heads. The percentage errors for the groundwater heads on the validation run were all within ±20%, which were acceptable for the purpose of this study.

To further analyze the accuracy of the groundwater flows, the observed observations were plotted against simulated observations resulting in Figure 9. The root mean square was calculated to be 54.38 ft which represents the average difference of the actual observation points in terms of residuals, how much higher or lower than the observed observations.

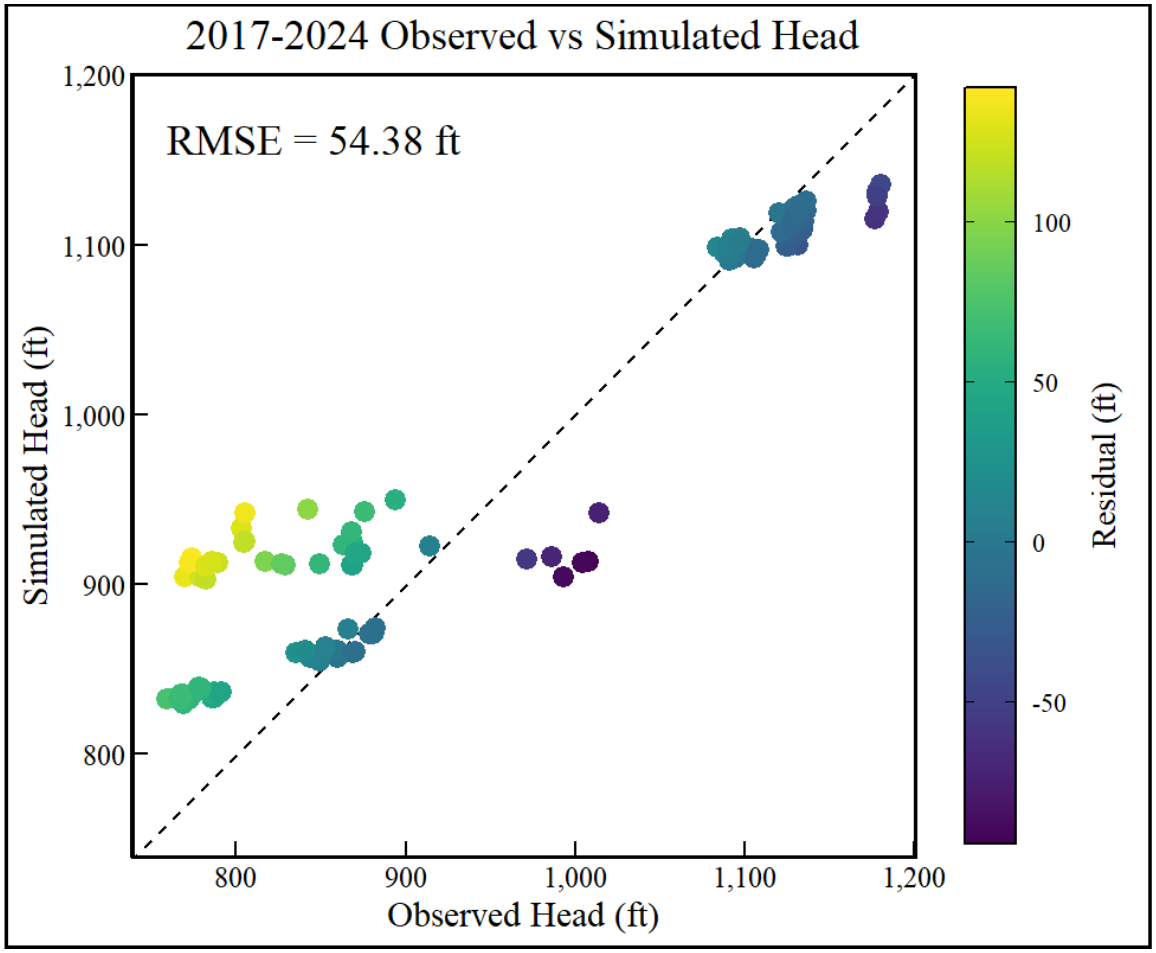

Figure 9. Observed heads plotted against simulated heads. The Root Mean Square Error was 54.38 ft across all years. More wells tended to be overestimated (simulating higher head) rather than underestimated (simulating lower head).

2.8 MT3D-USGS: Solute Transport

MT3D-USGS is a program that simulates solute transport within MODFLOW incorporating advection, dispersion, sink and source, and chemical reactions in simulations and more. The program needed the following data: porosity, bulk density, soil distribution/partitioning coefficients, initial concentrations, longitudinal dispersity, and diffusion coefficients.

2.8.1 Bulk Density

Bulk densities were retrieved from an ArcGIS Pro from a layer called CA_Soils[49]. It contains soil information for California intended for compliance with the Construction General Permit. An overview of the varying bulk densities in ng/ft^3 for the study area is illustrated in Figure 10.

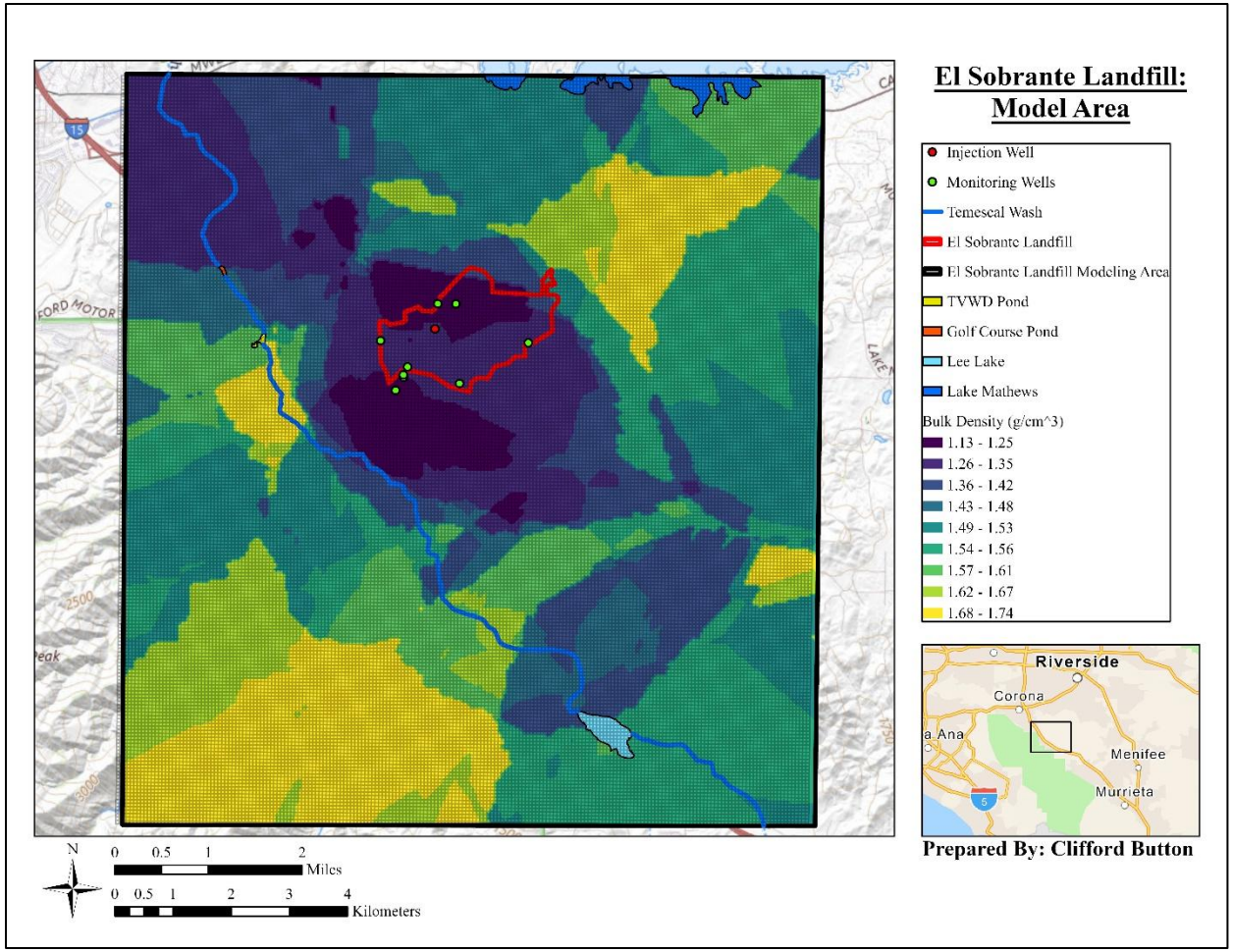

Figure 10. Bulk density of the study area represented in g/cm^3. The bulk densities were taken from an ArcGIS database with different soil parameters across the state of CA known as CA_Soils and interpolated for the study area using kriging for heterogeneity. Darker colors such as purple represent a lower bulk density, whereas lighter colors such as yellow represent higher bulk densities.

2.8.2 Soil Distribution Coefficient

In MT3D-USGS, the sorption model used was the linear isotherm which assumes that there is a linear relationship between the sorbed and dissolved concentrations of a solute, which in this case is PFAS. The sorption parameter in MODFLOW is the soil distribution coefficient/partition coefficient, k_d, which was calculated using Equation 2

$$k_d = f_{oc} \times K_{oc} \quad (2)$$

where k_d is the soil distribution coefficient, f_{oc} is the fraction of organic carbon, and K_{oc} is the organic carbon to water partition coefficient. f_{oc} values were calculated using Equation 3

$$f_{oc} = \frac{TOC\ \%}{100} \quad (3)$$

where TOC is the percentage of total organic carbon in the soil. TOC was calculated using Equation 4

$$TOC = \frac{SOM\ \%}{1.724} \quad (4)$$

where SOM is the percentage of soil organic matter in the soil and 1.724 is an assumption being that organic matter is made up of 50% carbon[50]. Using the United States Department of Agriculture's (USDA) Web Soil Survey, SOM data for the entire modeling area was obtained from two soil surveys[51]. The highest percentage of SOM was taken from both surveys, and an average was taken to find TOC and f_{oc}. It is assumed that these values represent the entire soil of the modeling area where SOM, TOC, and f_{oc} are 1.125%, 0.652%, and 6.52E-3, respectively.

K_{oc} values were retrieved from the EPA's CompTox Chemicals Dashboard which provides public access to chemistry, toxicity, and exposure data for a variety of chemicals[52]. K_{oc} values for the PFAS used in this study are summarized in Table 8 along with the f_{oc} and k_d values.

Table 8. K_{oc} and k_d values for different PFAS which were used in calculating retardation factors within MODFLOW. The f_{oc} was found to be 6.52E-3 which represented the entire model area (homogenous).

PFAS	K_{oc} (L/kg)	K_{oc} (ft^3/ng)	k_d (ft^3/ng)
PFOA	1,160	4.09E-11	2.67E-13
PFOS	1,460	5.15E-11	3.36E-13
PFNA	2,820	9.95E-11	6.49E-13
PFBA	89.10	3.14E-12	2.05E-14
PFBS	288.0	1.01E-11	6.59E-14
PFHxA	1,070	3.77E-11	2.46E-13
PFHxS	2,290	8.08E-11	5.27E-13
5:3 FTCA	871.0	3.07E-11	2.00E-13

2.8.3 Longitudinal Dispersivity and Diffusion Coefficients

Longitudinal dispersivity controls the spreading of a solute (PFAS in this case) in the direction of groundwater flow. Longitudinal dispersivity was calculated using the EPA's EPA On-line Tools for Site Assessment Calculation tool which is able to determine the longitudinal dispersivity based on the length of the plume[53]. Because the length of the plume is uncertain, it was assumed that the minimum length of the plume was the distance between the location of the injection well and the farthest monitoring well. The longitudinal dispersivity calculated was 42.8 ft.

Diffusion controls the movement of molecules from areas with higher concentrations to areas with lower concentrations. Diffusion coefficients for PFOA and PFOS were referenced using Schaefer et al. values for diffusion coefficients, whereas PFBS was calculated using linear interpolation of Damião et al. diffusion coefficients at 298.15 k[54,55]. The diffusion coefficients for PFOA, PFOS, and PFBS were 8.40E-10, 3.44E-10, and 7.75E-09, respectively.

2.8.4 PFAS Concentration Profiles

In ArcGIS Pro, the Inverse Distance Weighted (IDW) interpolation method was used for establishing the initial concentration files for the model. Due to the limited data regarding the number of samples recorded for different PFAS, the Kriging interpolation failed to estimate a semivariogram for the majority of the PFAS concentrations. Table 9 shows a breakdown of the number of PFAS samples taken at the landfill from both leachate and monitoring wells, ultimately showing the limited number of samples available for interpolation. One thing to note is that some of the monitoring well samples are from the same well.

Table 9. The number of samples taken of each PFAS from leachate and monitoring wells for the years of 2017 and 2022. No data existed for 5:3 FTCA in 2017 because it wasn't included in the sampling.

Year	PFAS Type	# of Leachate Samples	# of Monitoring Well Samples
2017	PFOA	3	6
2017	PFOS	2	3
2017	PFHxS	3	3
2017	PFNA	3	3
2017	PFBS	3	6
2017	PFBA	3	12
2017	PFHxA	3	5
2017	5:3 FTCA	0	0
2022	PFOA	2	4
2022	PFOS	2	4
2022	PFHxS	2	2
2022	PFNA	2	3
2022	PFBS	2	3
2022	PFBA	2	4
2022	PFHxA	2	4
2022	5:3 FTCA	2	4

3. Results & Discussion

There were 3 different scenarios, each running for 14 stress periods spanning from April 2017 through March 2125 in MODFLOW for PFAS transport.

3.1 Scenario 1 – PFOA & PFOS (Interpolated Concentration Profile)

Scenario 1 simulated PFOA and PFOS transport in the model area using IDW interpolated concentration profiles. This was under the assumption that the initial concentration of the modeling area was based on sampling data from monitoring wells at the landfill in 2017. These sampling points were interpolated over the modeling area to create an initial concentration profile to represent PFOA and PFOS spatially.

Figure 11(a) and (b) both illustrate the interpolated concentration profiles of PFOA and PFOS within the study area as described in Section 3.5. The results for PFOA and PFOS are shown in Figure 12(a)-(f) and Figure 13(a)-(f), respectively.

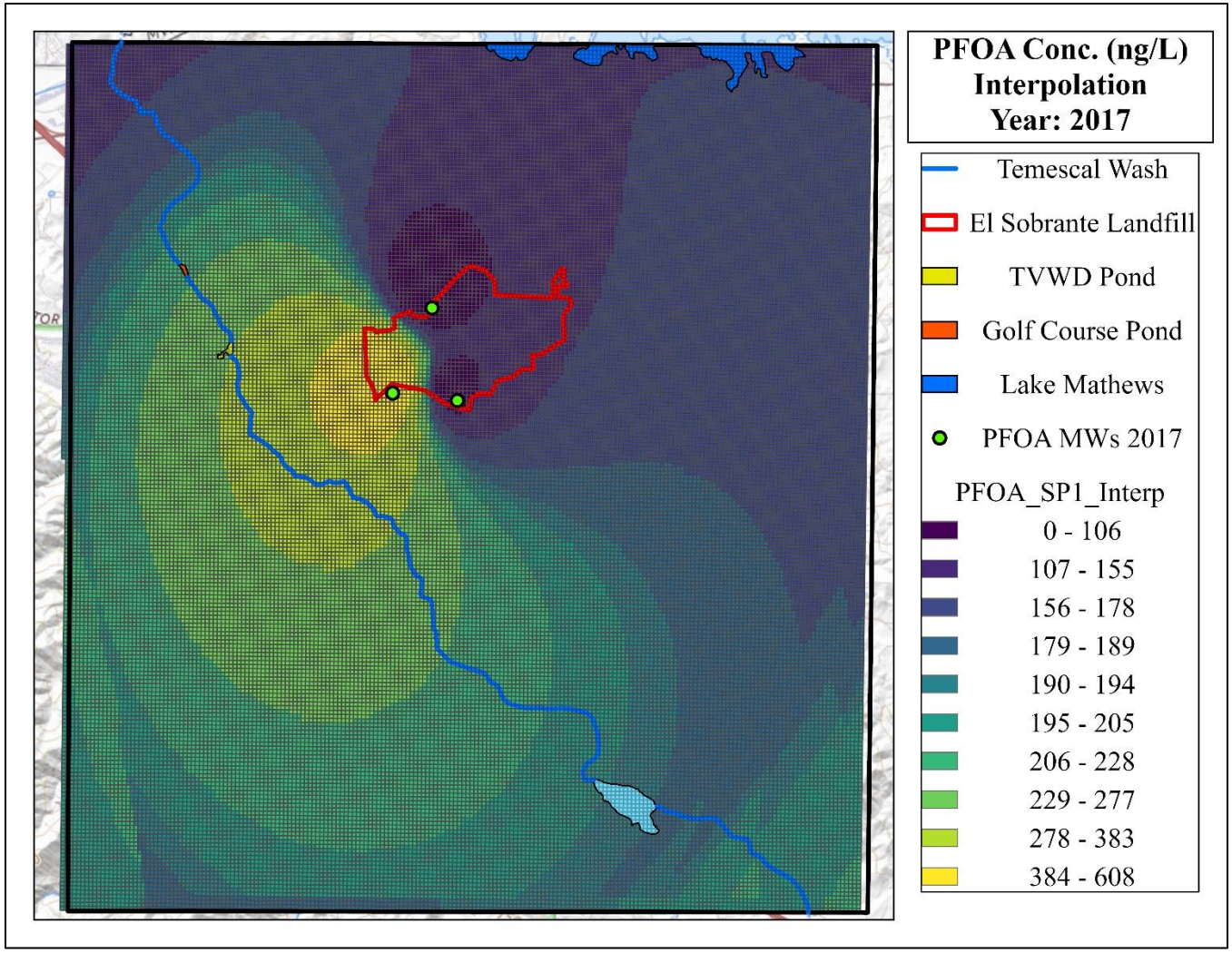

Figure 11(a). 2017 PFOA initial concentration profile using IDW interpolation. Only three monitoring wells detected PFOA which were used during interpolation. The highest concentration reported was about 608 ng/L.

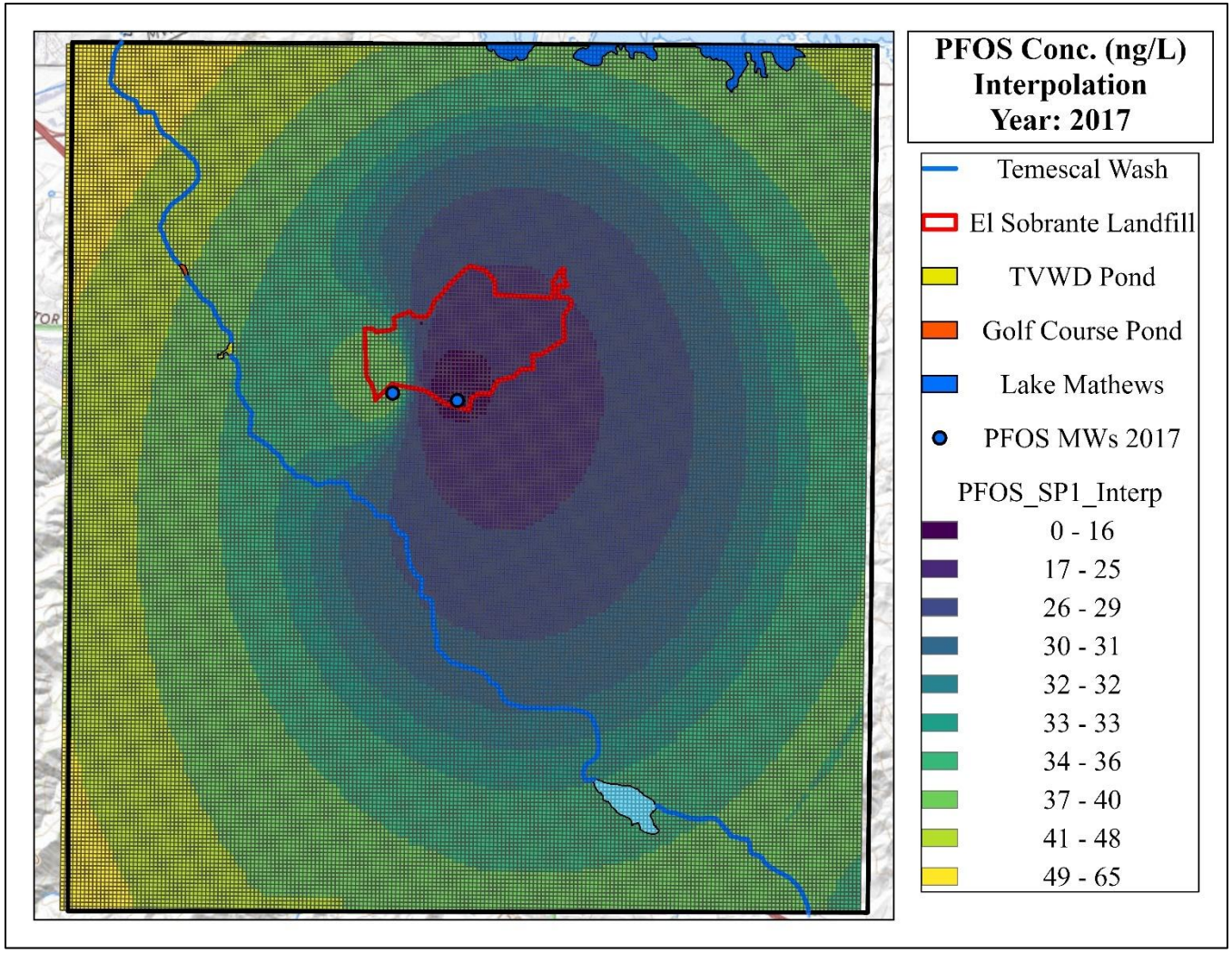

Figure 11(b). 2017 PFOS initial concentration profile using IDW interpolation. Only two monitoring wells detected PFOS which were used during interpolation. The highest concentration reported was about 65 ng/L.

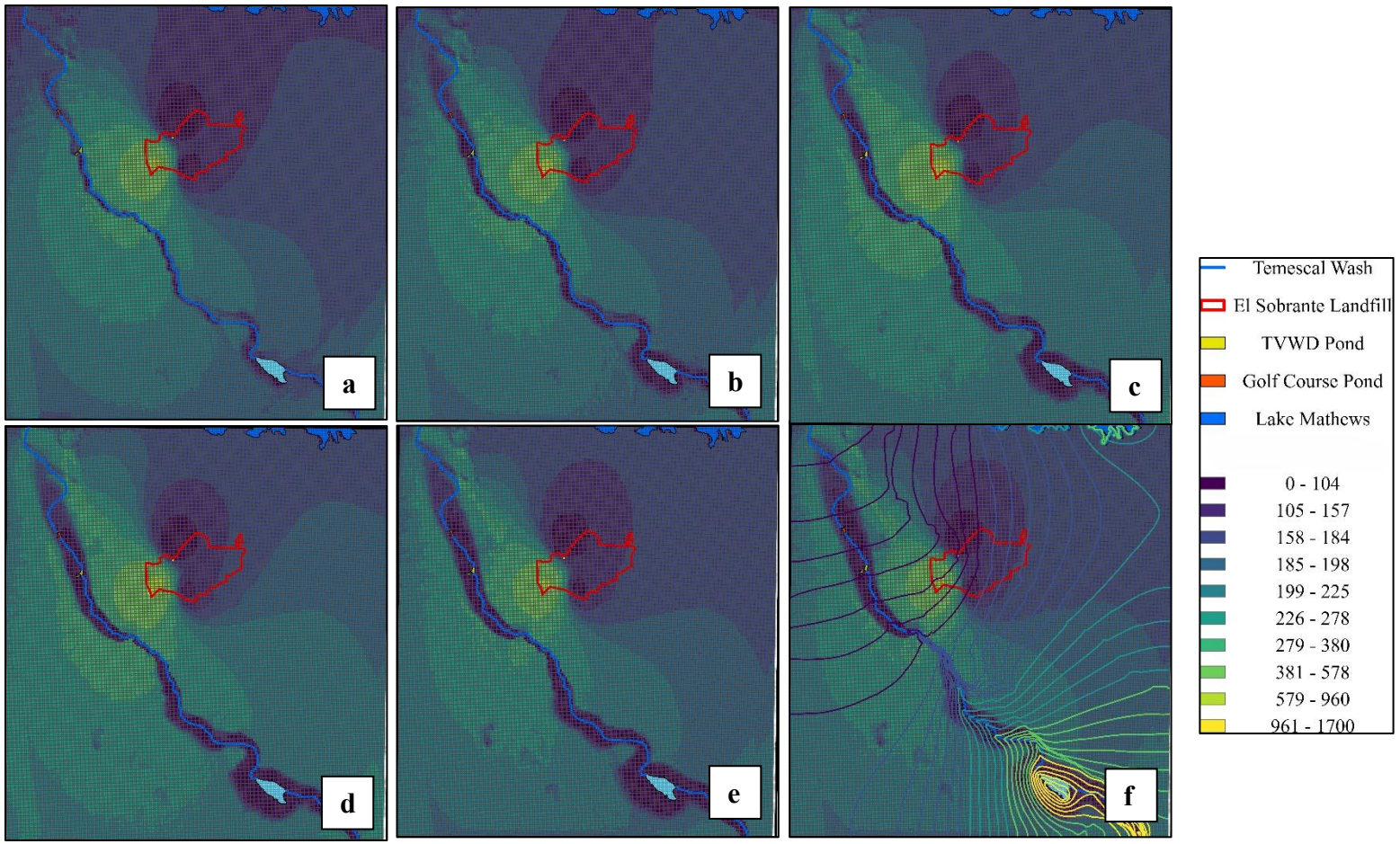

Figure 12(a)-(f). depict the concentration profiles of PFOA in ng/L representing 2025, 2045, 2065, 2085, 2105, and 2125, respectively. Figure 12(f) illustrates the concentration profile and the hydraulic gradient which demonstrates that the concentration plume does travel along the hydraulic gradient as expected. The darker areas represent lower concentrations, whereas lighter areas represent higher concentrations.

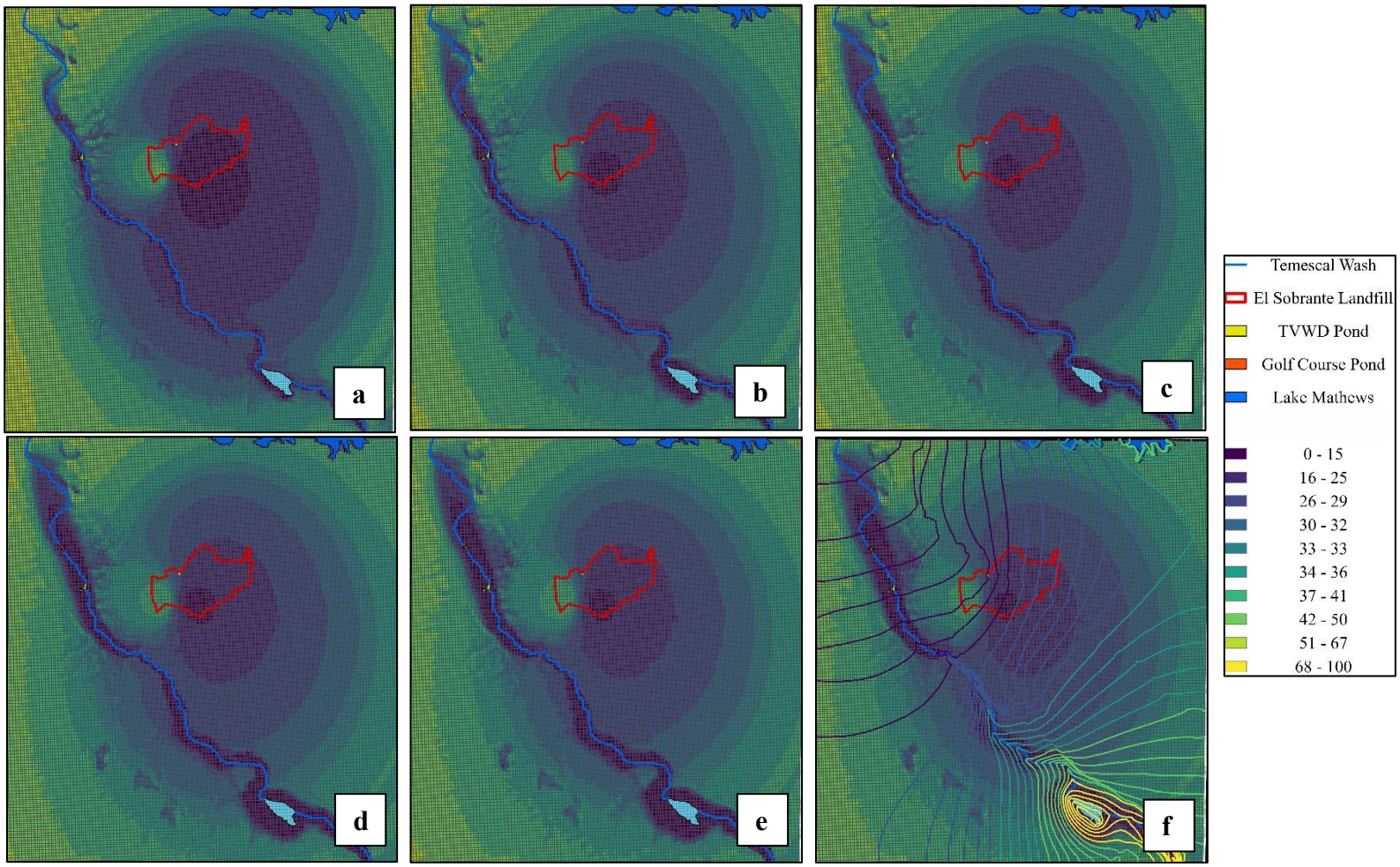

Figure 13(a)-(f). depicts the concentration profiles of PFOS in ng/L representing 2025, 2045, 2065, 2085, 2105, and 2125, respectively. Figure 13(f) illustrates the concentration profile and the hydraulic gradient which demonstrates that the concentration plume does travel along the hydraulic gradient as expected. The darker areas represent lower concentrations whereas lighter areas represent higher concentrations.

Both plumes move in the direction of the hydraulic gradient which is in the direction of northwest towards the Santa Ana River. The plume is also being discharged into the Temescal Creek which is highlighted in dark purple representing low concentrations. It is expected to be a sink for the plumes and eventually discharge into the Santa Ana River and/or different parts along the Temescal Creek. It is important to note that due to the absence of more PFOA and PFOS sampling data, the interpolation is likely overestimating the concentrations away from the landfill. PFOA and PFOS have 3 and 2 data points representing the entire model area, respectively. In addition, because there is limited data, interpolation had to be used in order to spatially calculate an initial concentration profile.

3.2 Scenario 2 – PFOA & PFOS (Initial Concentration = 0)

Scenario 2 simulated PFOA and PFOS transport in the model area, assuming that the initial concentration was zero or rather that there was no prior PFOA and PFOS contamination before 2017. The purpose of this scenario was to analyze the plume movements of both PFOA and PFOS from the landfill and determine the extent of each plume. The results for PFOA and PFOS are shown in Figure 14(a)-(f) and Figure 15(a)-(f), respectively.

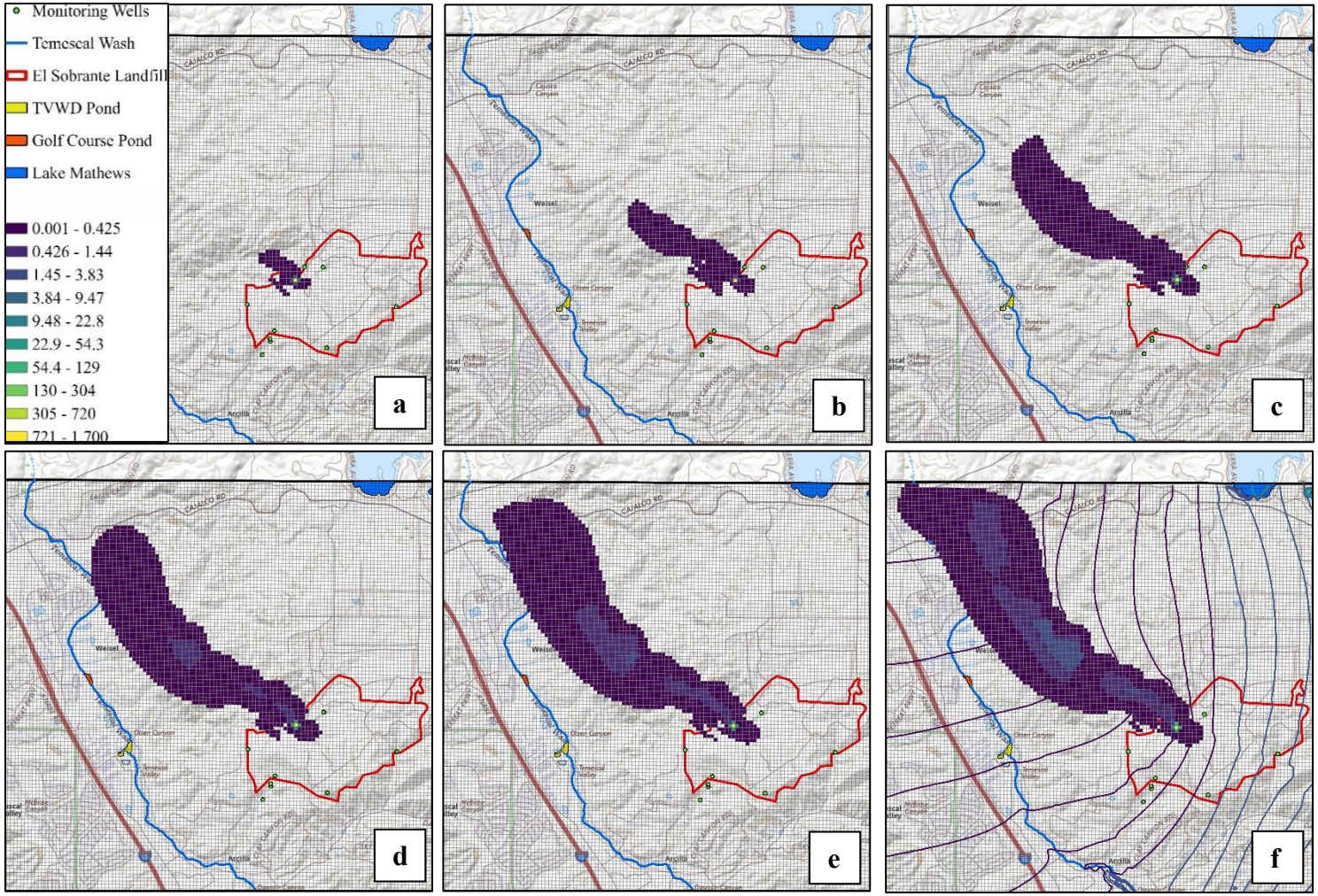

Figure 14(a)-(f). Represents the plume movement of PFOA in the years 2025, 2045, 2065, 2085, 2105, and 2125, respectively. The plume moves northwest towards the Temescal Creek and is expected to reach it by 2085. Darker areas represent lower concentrations, whereas lighter areas represent higher concentrations.

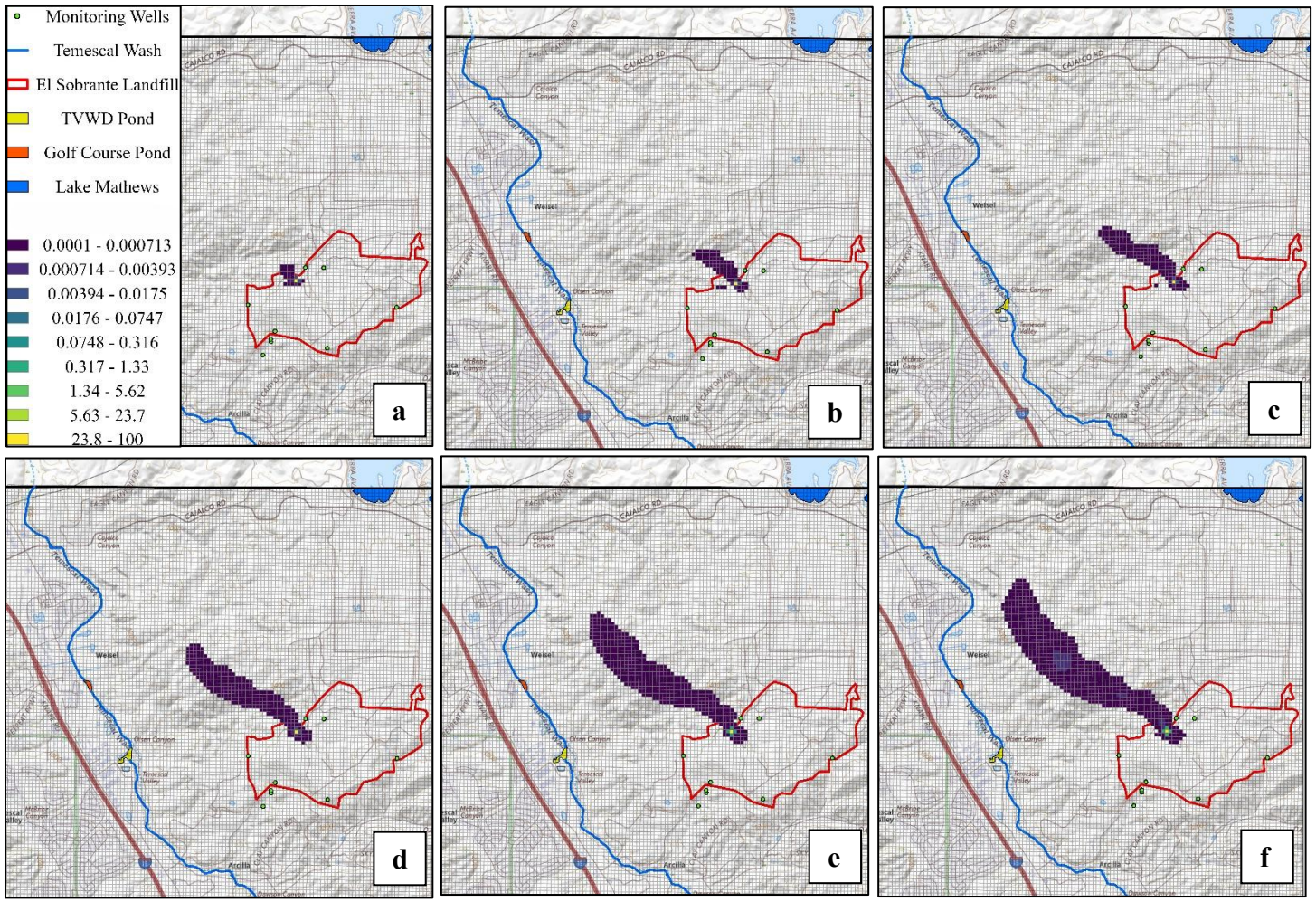

Figure 15(a)-(f). Represents the movement of PFOS in the years 2025, 2045, 2065, 2085, 2105, and 2125, respectively. The plume moves northwest towards the Temescal Creek and is not expected to reach it by 2125. Darker areas represent lower concentrations, whereas lighter areas represent higher concentrations.

After simulating for 108 years' worth of plume movement, PFOA traveled faster than PFOS did. Some factors that could have attributed to this are the concentrations of the injection well, the diffusion coefficients, and the soil distribution coefficients. Table 10 summarizes the injection well concentrations of PFOA and PFOS. These concentrations influence the increase in concentrations of the plume but not necessarily the shape or extent of the plume; however, the diffusion coefficients and soil distribution coefficients do.

Table 10. PFOA and PFOS injection well concentrations

Year	PFOA Leachate Conc. (ng/L)	PFOS Leachate Conc. (ng/L)
2017	26,000	230
2018	21,140	204
2019	16,280	178
2020	11,420	152
2021	6,560	126
2022	1,700	100
2023	1,700	100
2024	1,700	100

As mentioned before, PFOA and PFOS had diffusion coefficients of 8.40E-10 and 3.44E-10 ft^2/s, respectively, and soil distribution coefficients of are 2.67E-13 and 3.36E-13 ft^3/ng. A higher diffusion coefficient will lead to more spreading of the plume in contrast to a smaller diffusion coefficient which is demonstrated in Figure 14 (a)-(f) and Figure 15 (a)-(f). For the distribution coefficients, a higher value indicates slower plume movement where the contaminant adsorbs or sticks to soil particles whereas a lower value indicates faster plume movement and has less adsorption. This is demonstrated in Figure 14 (a)-(f) and Figure 15w (a)-(f). The soil distribution coefficient is related to the retardation factor,

R, which describes how fast or slow a contaminant will move in the groundwater based on interactions with the soil. Equation 5 illustrates the equation for the retardation factor:

$$R = 1 + \frac{\rho_b \times K_d}{\eta} \quad (5)$$

where, ρ_b is the bulk density of the soil (ng/ft^3), K_d, is the soil partitioning coefficient (ft^3/ng), η is the porosity (dimensionless), and R is the retardation factor (dimensionless). A retardation factor of 1 and greater than 1 means that the contaminant will move at the same speed as groundwater and slower than groundwater, respectively. A higher R represents higher adsorption with soil particles. MODFLOW calculates the retardation factor across the model area based on the input parameters.

3.3 Scenario 3 – PFBS (Effects of IDW, Kriging, and Natural Neighbor Interpolation)

Scenario 3 simulated PFBS transport in the model using the following interpolation methods for creating initial concentration profiles: IDW, Kriging, and Natural Neighbor. Three interpolation methods were chosen to determine the effectiveness each method had in simulating PFAS transport with very limited sampling data. These methods will be described in Section 3.4. A total of 4 simulations were ran, one assuming no initial concentration and the other three representing each of the different interpolation methods as described previously.

Figure 16 (a) and (b) illustrate the simulation run for 2017 and 2125 with no prior concentrations (initial concentration is zero in 2017) whereas Figure 17 (a)-(f) represents the simulation runs with the interpolated initial concentration profiles for 2017 and 2125.

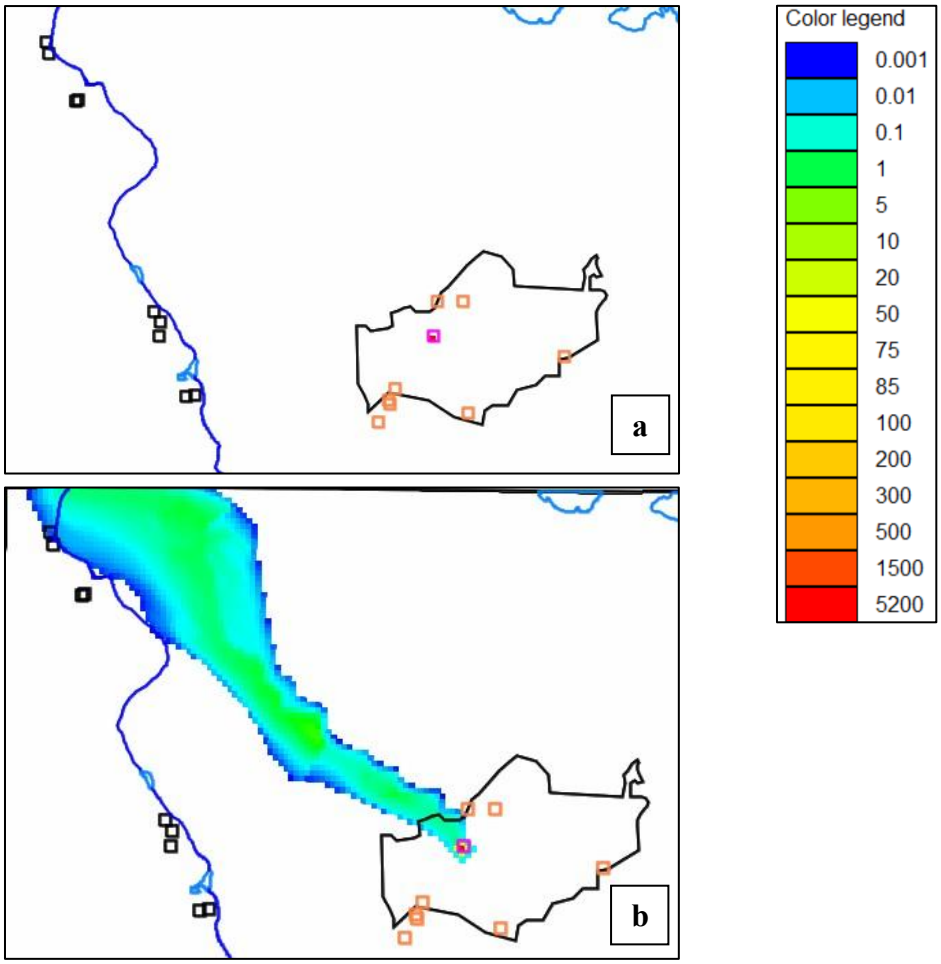

Figure 16(a) and (b). Represents 2017 (top) and 2125 (bottom) of PFBS transport in ng/L assuming no prior concentrations of PFBS are present. The PFBS plume is expected to reach the Temescal Creek by 2125.

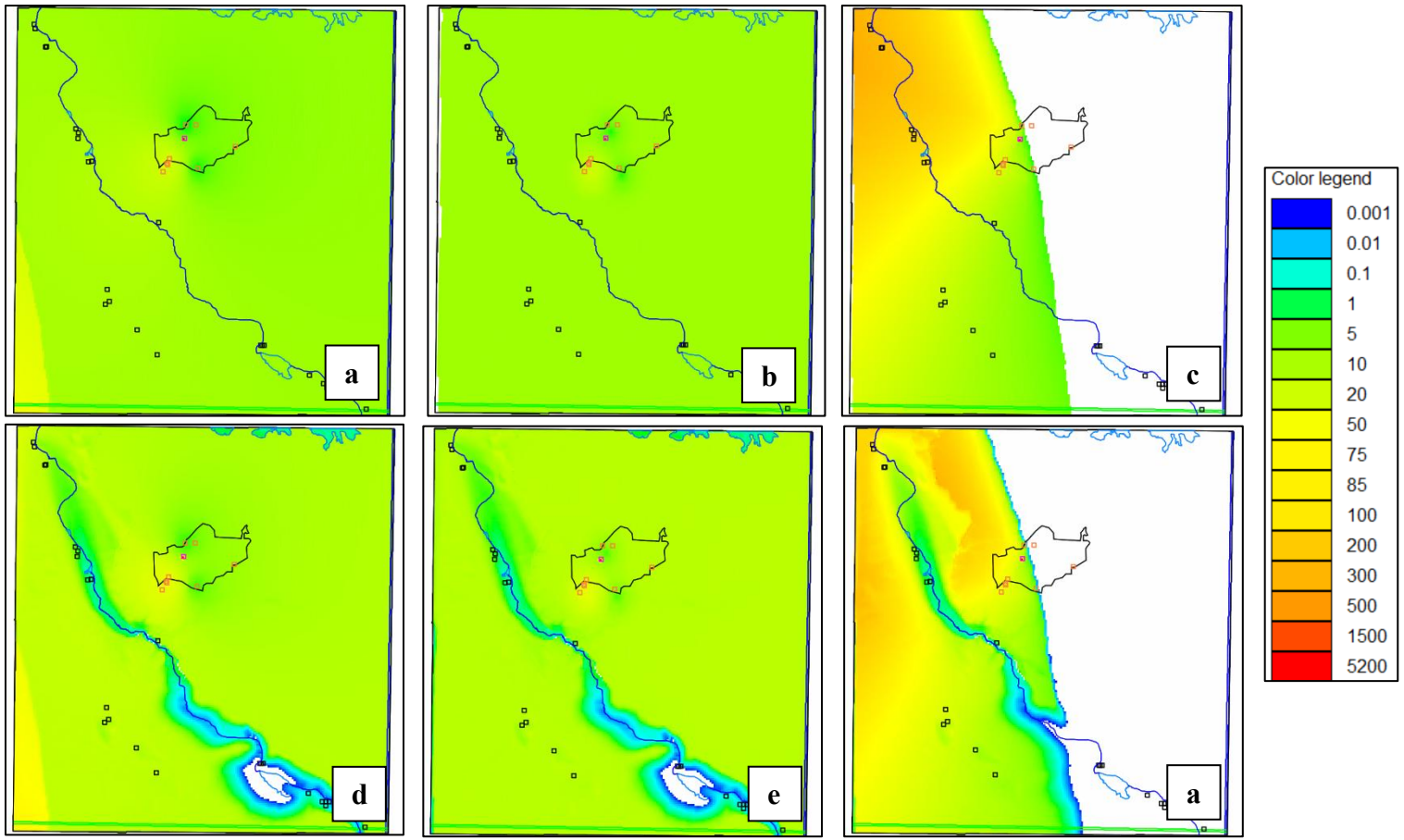

Figure 17 (a)-(f). Initial concentration profiles using interpolation methods: IDW (top and bottom left), Kriging (top and bottom middle), and Natural Neighbor (top and bottom right). The white portions of the figures represent anything less than 0.001 ng/L. IDW and Kriging interpolation methods are similar in terms of heterogeneity for concentration profiles; however, Natural Neighbor is different in terms of a higher initial concentration profile and no interpolation occurred to the right of the data points used for interpolation. The top images are 2017 and bottom images are 2125.

PFBS is considered a short chain PFAS where the carbon chain is less than 5 carbon atoms. Short chain PFAS are known to travel faster than long chain PFAS due to [cite source]. The diffusion coefficient and soil distribution coefficient of PFBS are 7.75E-09 ft^2/s and 6.59E-14 ft^3/ng, respectively. The diffusion coefficient is larger than PFOA and PFOS meaning it would spread more; however, the soil distribution coefficient is smaller than PFOA and PFOS meaning it would travel faster than both which is demonstrated in Figure 16 (b).

The interpolation methods differ slightly for IDW and Kriging; however, changes drastically with Natural Neighbor. Kriging works by using a geostatistical method that considers both the distance between the data and the spatial correlation which allows for a more accurate prediction. IDW works in a similar way where it only weighs the nearby points solely on distance. Natural Neighbor estimates values at unknown locations based solely on the values of known locations. The interpolation method creates shapes known as a Voronoi cell which cover the area closest to those points.

3.4 Data Availability

Because of the limited number of sampling data available at the landfill for PFAS concentrations, interpolation was required to create spatial concentration profiles of each PFAS to represent heterogeneity of varying concentrations. Had there been more sampling data available, interpolation would still be needed; however, it would not be as critical nor would it be very impactful. PEST would probably have been accurate in estimating the plume based on having more observation points to calibrate, specifically monitoring well observations for each PFAS. As mentioned previously in Table X, there

aren't many samples from monitoring wells in 2017 which is a big part of calibrating a solute transport model, more observation points mean a bigger range of parameter estimation.

Due to the limited amount of data available for PFAS concentrations, it was not possible to validate the PFAS plumes with only two points in time. Calibration for the contaminants could have been done with the two points in time (2017 and 2022); however, due to long computation times and limited storage space, it could not be done in this study. As stated previously, if more samples were taken in 2017 and 2022, a more accurate solute transport model could be achieved.

Simulating PFAS transport is crucial for understanding and estimating the extent of varying plumes. Because landfills are not regulated for PFAS, they are not required to meet a certain level of PFAS in the leachate. In addition, landfills are not 100% effective at capturing all leachate, posing a risk of groundwater contamination in the future. Though PFAS plumes move slowly over time and do not pose any significant risk today, it will eventually travel, accumulating more concentrated PFAS and potentially impacting local water supplies.

This research was aimed at understanding data gaps in creating a groundwater PFAS model; however, as demonstrated in this paper, the biggest gap in creating an efficient model is the number of sampling data. As said before, more sampling data can significantly increase the accuracy of PFAS plumes and groundwater tables. PFOA and PFBS only had three sampling points to conduct a spatial interpolation of the initial concentration profiles whereas PFOS only had two. This data is very limited and

underestimates the actual extent of PFAS in the groundwater. The most obvious solution to filling this gap is to drill more wells and increase the number of samples over time. However, the cost of drilling a well depends on many factors including the type of well casing, how deep the well is drilled, the types of soil that need to be drilled at (sand, clay, granite, boulders, etc.), and labor. These costs vary from $10,000 to $50,000+ for one well.

4. Conclusion

PFAS have and still are an issue regarding the risks of groundwater contamination. Because these chemicals take years to break down naturally, they may accumulate in groundwater and potentially contaminate drinking water sources. MODFLOW is a powerful tool for modeling groundwater and solute transport such as PFAS. This study focused on PFOA, PFOS, and PFBS as well as the efficiency of using different interpolation methods when there isn't enough data to estimate the initial extent of a PFAS plume. Kriging interpolation is more accurate in comparison to Natural Neighbor and IDW; however, it fails quickly when there are limited data points. IDW and Natural Neighbor excel when there are limited data points, but lack in accuracy when comparing to Kriging. IDW may overestimate concentrations across the entire interpolation area, whereas Natural Neighbor may underestimate concentrations and focus on areas with more points. The lack of PFAS sampling points decreases the accuracy of a groundwater solute model severely which should be an area of concern when trying to create a new PFAS groundwater model.

References

(1) US EPA, O. *Per- and Polyfluoroalkyl Substances (PFAS)*. https://www.epa.gov/sdwa/and-polyfluoroalkyl-substances-pfas (accessed 2025-01-23).

(2) Buck, R. C.; Franklin, J.; Berger, U.; Conder, J. M.; Cousins, I. T.; De Voogt, P.; Jensen, A. A.; Kannan, K.; Mabury, S. A.; Van Leeuwen, S. P. Perfluoroalkyl and Polyfluoroalkyl Substances in the Environment: Terminology, Classification, and Origins. *Integrated Environmental Assessment and Management* **2011**, *7* (4), 513–541. https://doi.org/10.1002/ieam.258.

(3) *Organofluorine Chemistry: Principles and Commercial Applications*; Banks, R. E., Smart, B. E., Tatlow, J. C., Eds.; Springer US: Boston, MA, 1994. https://doi.org/10.1007/978-1-4899-1202-2.

(4) Lindstrom, A. B.; Strynar, M. J.; Libelo, E. L. Polyfluorinated Compounds: Past, Present, and Future. *Environ. Sci. Technol.* **2011**, *45* (19), 7954–7961. https://doi.org/10.1021/es2011622.

(5) Whitehead, H. D.; Venier, M.; Wu, Y.; Eastman, E.; Urbanik, S.; Diamond, M. L.; Shalin, A.; Schwartz-Narbonne, H.; Bruton, T. A.; Blum, A.; Wang, Z.; Green, M.; Tighe, M.; Wilkinson, J. T.; McGuinness, S.; Peaslee, G. F. Fluorinated Compounds in North American Cosmetics. *Environ. Sci. Technol. Lett.* **2021**, *8* (7), 538–544. https://doi.org/10.1021/acs.estlett.1c00240.

(6) Kotthoff, M.; Müller, J.; Jürling, H.; Schlummer, M.; Fiedler, D. Perfluoroalkyl and Polyfluoroalkyl Substances in Consumer Products. *Environ Sci Pollut Res* **2015**, *22* (19), 14546–14559. https://doi.org/10.1007/s11356-015-4202-7.

(7) Wang, Z.; DeWitt, J. C.; Higgins, C. P.; Cousins, I. T. A Never-Ending Story of Per- and Polyfluoroalkyl Substances (PFASs)? *Environ. Sci. Technol.* **2017**, *51* (5), 2508–2518. https://doi.org/10.1021/acs.est.6b04806.

(8) U.S. Environmental Protection Agency; Office of Water (4304T); Office of Science and Technology; Health and Ecological Criteria Division; Washington, DC 20460. Drinking Water Health Advisory: Hexafluoropropylene Oxide (HFPO) Dimer Acid (CASRN 13252-13-6) and HFPO Dimer Acid Ammonium Salt (CASRN 62037-80-3), Also Known as “GenX Chemicals.”

(9) US EPA, O. *Our Current Understanding of the Human Health and Environmental Risks of PFAS*. https://www.epa.gov/pfas/our-current-understanding-human-health-and-environmental-risks-pfas (accessed 2025-01-27).

(10) Barry, V.; Winquist, A.; Steenland, K. Perfluorooctanoic Acid (PFOA) Exposures and Incident Cancers among Adults Living Near a Chemical Plant. *Environ Health Perspect* **2013**, *121* (11–12), 1313–1318. https://doi.org/10.1289/ehp.1306615.

(11) Vélez, M. P.; Arbuckle, T. E.; Fraser, W. D. Maternal Exposure to Perfluorinated Chemicals and Reduced Fecundity: The MIREC Study. *Human Reproduction* **2015**, *30* (3), 701–709. https://doi.org/10.1093/humrep/deu350.

(12) Ahrens, L.; Shoeib, M.; Harner, T.; Lee, S. C.; Guo, R.; Reiner, E. J. Wastewater Treatment Plant and Landfills as Sources of Polyfluoroalkyl Compounds to the Atmosphere. *Environ. Sci. Technol.* **2011**, *45* (19), 8098–8105. https://doi.org/10.1021/es1036173.

(13) Coffin, E. S.; Reeves, D. M.; Cassidy, D. P. PFAS in Municipal Solid Waste Landfills: Sources, Leachate Composition, Chemical Transformations, and Future Challenges. *Current Opinion in Environmental Science & Health* **2023**, *31*, 100418. https://doi.org/10.1016/j.coesh.2022.100418.

(14) Koda, E.; Grzyb, M.; Osiński, P.; Vaverková, M. D. Analysis of Failure in Landfill Construction Elements. *MATEC Web Conf.* **2019**, *284*, 03002. https://doi.org/10.1051/matecconf/201928403002.

(15) Mitchell, J. K.; Seed, R. B.; Seed, H. B. Kettleman Hills Waste Landfill Slope Failure. I: Liner-System Properties. *Journal of Geotechnical Engineering* **1990**, *116* (4), 647–668. https://doi.org/10.1061/(ASCE)0733-9410(1990)116:4(647).

(16) Lang, J. R.; Allred, B. M.; Field, J. A.; Levis, J. W.; Barlaz, M. A. National Estimate of Per- and Polyfluoroalkyl Substance (PFAS) Release to U.S. Municipal Landfill Leachate. *Environ. Sci. Technol.* **2017**, *51* (4), 2197–2205. https://doi.org/10.1021/acs.est.6b05005.

(17) Raschke, A.; Nejadhashemi, A. P.; Rafiei, V.; Fernandez, N.; Shabani, A.; Li, S.-G. Opportunities and Challenges of Integrated Large-Scale PFAS Modeling: A Case Study for PFAS Modeling at a Watershed Scale. *Journal of Environmental Engineering* **2022**, *148* (9), 05022005. https://doi.org/10.1061/(ASCE)EE.1943-7870.0002034.

(18) Engers, A. J. Estimating Historical Concentrations of Per- and Polyfluoroalkyl Substances with Groundwater Flow and Transport Models and a Monte Carlo Analysis. M.S., Colorado School of Mines, United States -- Colorado, 2021. https://www.proquest.com/docview/2578153624/abstract/16B30B9C909C4C51PQ/1 (accessed 2025-01-27).

(19) Gefell, M. J.; Huang, H.; Opdyke, D.; Gustafson, K.; Vlassopoulos, D.; McCray, J. E.; Best, S.; Carey, M. Modeling PFAS Fate and Transport in Groundwater, with and Without Precursor Transformation. *Groundwater* **2022**, *60* (1), 6–14. https://doi.org/10.1111/gwat.13152.

(20) *El Sobrante*. https://www.wm.com/location/california/inland-empire/el-sobrante/el-sobrante.jsp (accessed 2025-02-24).

(21) *The National Map - Data Delivery | U.S. Geological Survey*. https://www.usgs.gov/the-national-map-data-delivery (accessed 2025-02-24).

(22) *California's Groundwater Live: Groundwater Levels*. ArcGIS StoryMaps. https://storymaps.arcgis.com/stories/b3886b33b49c4fa8adf2ae8bdd8f16c3 (accessed 2025-02-24).

(23) *Well Completion Report Map Application*. https://dwr.maps.arcgis.com/apps/webappviewer/index.html?id=181078580a214c0986e2da28f8623b37 (accessed 2025-02-24).

(24) *StructX - Soil Properties*. https://structx.com/Soil_Properties.html (accessed 2025-05-14).

(25) *Hydraulic Conductivity and Permeability of Various Soil Types*. https://structx.com/Soil_Properties_007.html (accessed 2025-02-24).

(26) *Porosity Values for Various Soil Types*. https://structx.com/Soil_Properties_006.html (accessed 2025-02-24).

(27) *Hydraulic Properties :. Aquifer Testing 101*. http://www.aqtesolv.com/aquifer-tests/aquifer_properties.htm (accessed 2025-02-24).

(28) *How Kriging works—ArcGIS Pro | Documentation*. https://pro.arcgis.com/en/pro-app/latest/tool-reference/spatial-analyst/how-kriging-works.htm (accessed 2025-03-05).

(29) *Temescal C AB Main ST a Corona CA*. https://waterdata.usgs.gov/monitoring-location/11072100/ (accessed 2025-05-14).

(30) *Temescal C a Corona LK NR Corona CA*. https://waterdata.usgs.gov/monitoring-location/11071900/ (accessed 2025-05-14).

(31) *Lake Mathews Reservoir Report | California Dams & Reservoirs*. Snoflo Climate Research. https://snoflo.org/reservoir/california/lake-mathews (accessed 2025-05-14).

(32) *Rainfall Map*. https://content.rcflood.org/RainfallMap/ (accessed 2025-02-24).

(33) *GeoTracker PFAS Map*. https://geotracker.waterboards.ca.gov/map/pfas_map (accessed 2025-02-24).

(34) *GAMA Groundwater*. https://gamagroundwater.waterboards.ca.gov/gama/gamamap/public/ (accessed 2025-02-24).

(35) 12.02001.Pdf. https://media.rivcocob.org/proceeds/2019/p2019_12_17_files/12.02001.pdf (accessed 2025-05-14).

(36) 2023 El Sobrante Landfill Final Annual Report_website.Pdf. https://rcwaste.org/sites/g/files/aldnop376/files/users/user86/2023%20El%20Sobrante%20Landfill%20Final%20Annual%20Report_website.pdf (accessed 2025-05-14).

(37) Portals-0-Files-ElSobrante-2020-FINAL-20-2019-El-Sobrante-Landfill-Annual-Status-Report.Pdf. https://rcwaste.org/sites/g/files/aldnop376/files/migrated/Portals-0-Files-ElSobrante-2020-FINAL-20-2019-El-Sobrante-Landfill-Annual-Status-Report.pdf (accessed 2025-05-14).

(38) Portals-0-Files-ElSobrante-2021-Final-202020-20Annual-20Report--20El-20Sobrante-20Landfill.Pdf. https://rcwaste.org/sites/g/files/aldnop376/files/migrated/Portals-0-Files-ElSobrante-2021-Final-202020-20Annual-20Report--20El-20Sobrante-20Landfill.pdf (accessed 2025-05-14).

(39) Portals-0-Files-ElSobrante-2022-Final-202021-20El-20Sobrante-20Annual-20Reports.Pdf. https://rcwaste.org/sites/g/files/aldnop376/files/migrated/Portals-0-Files-ElSobrante-2022-Final-202021-20El-20Sobrante-20Annual-20Reports.pdf (accessed 2025-05-14).

(40) Wampler, K. 3. DISCUSSION ITEMS A. Staff Update.

(41) Exhibit-10---El-Sobrante-Landfill-Declaration-of-David-Meyer-Re-Regular-Variance.Pdf.

(42) *Assessment of Municipal Solid-Waste Landfill Liner Performance*. https://doi.org/10.1061/JOEEDU.EEENG-7218.

(43) *MODFLOW and Related Programs | U.S. Geological Survey*. https://www.usgs.gov/mission-areas/water-resources/science/modflow-and-related-programs (accessed 2025-05-15).

(44) *MODFLOW 6: USGS Modular Hydrologic Model | U.S. Geological Survey*. https://www.usgs.gov/software/modflow-6-usgs-modular-hydrologic-model (accessed 2025-05-15).

(45) *ModelMuse: A Graphical User Interface for Groundwater Models | U.S. Geological Survey*. https://www.usgs.gov/software/modelmuse-a-graphical-user-interface-groundwater-models (accessed 2025-05-15).

(46) PESTMAN.Pdf. https://www.epa.gov/sites/default/files/documents/PESTMAN.PDF (accessed 2025-05-21).

(47) Anderson, M. P.; Woessner, W. W.; Hunt, R. J. *Applied Groundwater Modeling: Simulation of Flow and Advective Transport*, Second edition.; Academic Press: London ; San Diego, CA, 2015.

(48) Gavin, H. P. The Levenberg-Marquardt Algorithm for Nonlinear Least Squares Curve-Fitting Problems. **2024**.

(49) *CA Soils - Overview*. https://www.arcgis.com/home/item.html?id=9a5fb48363e54dfebc34b12e806943b7&view=list&sortOrder=desc&sortField=defaultFSOrder#overview (accessed 2025-05-25).

(50) Chon, N. Q. The Role of Soil Organic Carbon.

(51) *Web Soil Survey - Home*. https://websoilsurvey.nrcs.usda.gov/app/ (accessed 2025-05-25).

(52) *CompTox Chemicals Dashboard*. https://comptox.epa.gov/dashboard/ (accessed 2025-05-24).

(53) *EPA On-line Tools for Site Assessment Calculation | Ecosystems Research | US EPA*. https://www3.epa.gov/ceampubl/learn2model/part-two/onsite/longdisp.html (accessed 2025-06-12).

(54) Schaefer, C. E.; Drennan, D.; Nickerson, A.; Maizel, A.; Higgins, C. P. Diffusion of Perfluoroalkyl Acids through Clay-Rich Soil. *Journal of Contaminant Hydrology* **2021**, *241*, 103814. https://doi.org/10.1016/j.jconhyd.2021.103814.

(55) Damião, G.; Morgado, P.; Silva, P.; Martins, L. F. G.; MCabe, C.; Filipe, E. J. M. Perfluorinated Pollutants in Water: Diffusion Coefficient of Perfluorosulfonic Acids by Molecular Dynamics Simulations. *Fluid Phase Equilibria* **2023**, *575*, 113928. https://doi.org/10.1016/j.fluid.2023.113928.